# Power optimization of wind farms by curtailment of upwind turbines

Simon Kirkeby Wessel


Kongens Lyngby 2015

Technical University of Denmark
Department of Applied Mathematics and Computer Science
Richard Petersens Plads, building 324,
2800 Kongens Lyngby, Denmark
Phone +45 4525 3031
compute@compute.dtu.dk
www.compute.dtu.dk

# Summary (English)

Renewable energy is getting more popular and accounts for an increasing part of the annual energy production in Denmark. Wind energy is one the more prominent ways of producing renewable energy. Wind turbines are often placed together in wind farms, which often are placed off-shore. Collecting turbines in wind farms has the drawback of causing wake effects, which significantly decrease the efficiency of wind farm.

This report presents a method to limit the wake effects of wind farms by optmising the set point distribution given to all the wind turbines in a wind farm. Curtailing upwind turbines is shown to increase the total power production of wind farms of different size and shape. Several methods to optimise the set point distributions are presented to give robust solutions, as the optimised objective function contains local optmisers.

It is calculated how much the power production can be increased by curtailing upwind turbines. It is shown that the annual power production for a square wind farm consisting of 25 turbines can be increased 1.77% when curtailing upwind turbines compared to more naive strategies. This number is shown to be dependent on the shape of the wind farm as the increase for a fan-shaped wind farm is only 1.05%.

# Summary (Danish)

Vedvarende energi bliver mere populært og står for en stigende del af den danske årlige energi produktion. Vind energi er en af de mest fremtrædende måder til at producere vedvarende energi. Vind turbiner bliver ofte samlet i vindfarme, der ofte er placeret på havet. En ulempe ved at samle turbine i vindfarme er at wake-effekter opstår, og reducerer virkningsgraden af vindfarmen betydeligt.

Denne rapport præsenterer en metode til at begrænse wake-effekterne af vindfarme ved, at optimere setpunkter givet til alle turbiner i en vindfarm. Ved at begrænse foranstående (i forhold til vindretning) turbine bliver det vist, at en total energi produktion kan øges for vindfarme af forskellige størrelser og form. Flere metoder til at optimere setpunktsfordelinger bliver præsenteret for at give en robust løsning, eftersom den optimerede objectfunktion indeholder local optimisers.

Det bliver udregnet hvor meget energi produktionen kan forøges ved at begrænse foranstående turbine. Det bliver vist at den årlige energi produktion for en kvadratisk vindfarm bestående af 25 turbiner kan øges med 1.77%, når foranstående turbiner begrænses sammenlignet med en simplere strategi. Dette tal bliver vist at være afhængigt af formen på vindfarmen, eftersom forøgningen i energi produktion for en vifte-formet vindfarm kun er 1.05 %.

# Preface

This thesis is submitted at Technical University of Denmark to fulfill the requirements for acquiring the degree Master of Science in Mathematical Modeling and Computing.

This thesis has been written at DTU Compute Department of Applied Mathematics and Computer Science from the 16th of September 2014 and to the 31st of January 2015, and accounts for 30 ECTS poitns. The work has be done under supervision from Lasse Engbo Christiansen Associate professor, Niels Kjølstad Poulsen Associate professor from Department of Applied Mathematics and Computer Science, and Mahmood Mirzaei Postdoc from Department of Wind Energy. Two external supervisors, Klaus Baggesen Hilger and Lars Henrik Hansen from DONG Energy Wind Power, department of Business Modelling, have also been associated with the formation of this thesis.

Lyngby, 31-January-2015

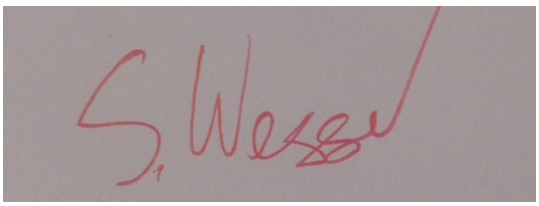

Simon Kirkeby Wessel

# Acknowledgements

I would like to use this opportunity to thank my supervisors at DTU: Lasse Engbo Christiansen, Niels Kjølstad Poulsen and Mahmood Mirzaei, for offering guidance, valuable discussions and constructive criticism for the last five months. I'm also grateful for the interest taken in this project by Lars Henrik Hansen and Klaus Baggesen Hilger from DONG Energy, given the report a broader perspective.

I would also like to thank my family and closest peers for being patient, and providing support during the project. A gratitude is given to my study group for discussing relevant matters and providing new perspectives to the project.

Pierre-Elouan Rethore, DTU Department of Wind Energy, should also be acknowledge for proving a solid and highly appreciated framework for a Matlab implementation of the Jensen wake model.

# Contents

Chapter 1

# Introduction

In the last decades an increased focus has been on renewable energy to decrease the use of fossil fuels. Wind energy is one of the most progressive types of renewable energy. Wind turbines are often placed in wind farms both off-shore and on-shore. However, grouping the turbines in farms has the downside of increased wake effects. Wind turbine wakes are the wind fields behind turbine rotors with a reduced wind speed. As they significantly reduce the efficiency of wind farms, wakes have been a topic for many research papers in the last decades.

Reducing the wake effects for wind farms would increase their efficiency and make wind energy more competitive. Wake effects can be reduced in many way e.g. by making better turbine designs, optimising wind farm layouts, or improve the controlling of the wind farm. The design and gearing of turbines has not been considered in this report, but wind farms layouts are analysed and two control strategies are defined and compared.

The wake effects has to be modelled before the controlling of wind farms can be optimised. The wake effects are extremely difficult to model accurately as they are characterised by unstable wind flows. The research on wake effects has given a wide range of model to describe the wakes which varies a lot in complexity. Some models are very simple while others are very detailed requiring high performance computers to be used.

The main goal of this report is to analyse the performance of two different control strategies for wind farms. Many control strategies consider fatigue loads on turbines though, which will not be addressed in this report. Before it is possible to evaluate control strategies, the wake effects for wind turbines must be quantified.

## Report outline

### Aerodynamics of individual wind turbines

This chapter gives a brief introduction to the aerodynamics affecting wind turbines. The turbine model used in this report is also defined in this chapter, together with a description of the controlling of the turbine.

### Wake effects from wind turbines

The aerodynamics affecting wakes are described in this chapter and an general introduction to wake models is given. The wake model used in report is presented in details as well.

### Optimizing set point distributions for row wind farms

A control strategy for increasing the power production is defined and analysed for row wind farms. Methods to overcome issues, with the optimised objective function, are proposed.

### Wind farms in two dimensions

In this chapter, the control strategy for improved power production will be tested on wind farms in two dimensions. The control strategy is compared to simpler more naive control strategy.

### Sensitivity analysis and structural changes

The method to optimise the set point distributions are tested for a new kind of turbine and tested on a more complex wind farm layout. Sensitivity to wind direction is also tested in this chapter.

### Economical effects of curtailing upwind turbines

The annual power production of wind farms is calculated and the economical gain from using the improved control strategy is presented.

Chapter 2

# Aerodynamics of individual wind turbines

To model a wind turbine the aerodynamics of the wind flow when hitting a wind turbine must be described to some extent. Describing the wind field passing through a rotor is considered a difficult task. This task can luckily be reduced in complexity by only considering certain factors. For this chapter only the 2D aerodynamics are described while assuming the wind flow is stationary, incompressible and frictionless.

## 2.1 2D aerodynamics for wind turbines

This section will give a summary of the most important forces acting on the blades of the turbine. Chapter 2, 3 and 4 from Hansen (2008)[Han08] have been used as background material for this and the following section and will not be quoted continuously in these sections. Wind turbines obviously work by the blades extracting kinetic energy from the wind. In other words, the wind is exerting a force on blades making them rotate. The force acting on the blade is described in the 2D rotor plane.

Figure 2.1 shows a simple drawing of a turbine blade seen from the center of the

rotor in the rotor plane. The force, $F$, acting on the blade, is decomposed into two directions, one perpendicular to wind and one parallel to the wind. The perpendicular force is called the lift and the parallel force is called drag. Both the drag, $D$, and the lift, $L$, are shown on the figure parallel to the the x- and y-axis, respectively.

The drag force is pushing the turbine in the direction of the wind and the lift is making the rotor rotate allowing the turbine to produce energy. When considering a wind turbine it is desirable to have the drag as small as possible, while the lift should be as large as possible to increase the power production.

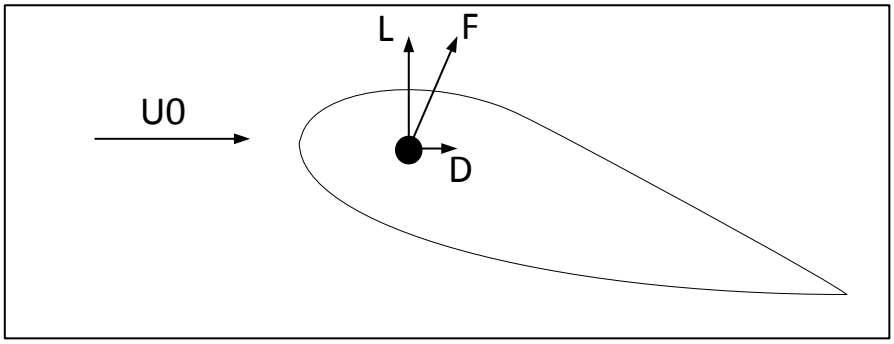


**Figure 2.1:** Two dimensional drawing of forces acting on a wind turbine blade.

When the wind hits the blade, making it rotate, a difference in pressure above and below the blade is generated. This difference in pressure is the reason for force acting on the blade. The pressure above the blade is lower than below giving mainly a lift component, when the blade is aligned with the wind. The only drag from pressure in this case comes from friction between the air and the blade. As long as the boundary layer between the airfoil and the air is attached to the blade the flow behind the blade is said to be laminar, meaning no turbulence is in introduced. When the angle of the blade increases, the boundary layer might separate from the blade and turbulent flow starts to occur, which increases the drag.

It is favorable to have the separation of the boundary layer starting at the trailing point of blade and move toward the leading point, since this will cause the drag force to increase slowly when the angle between the wind and blade increases. If the separation of the boundary layer happened all over the upper side of the blade, for a small changes in the angle, the drag would increase dramatically, which is undesirable.

The aerodynamics of the blade have only been considered in 2D in this report. A note on one of the results from 3D aerodynamics needs to be made, though. 3D vortexes are introduced, when analysing the 3D aerodynamics of a turbine blade, changing the angle of attack between the wind and the blade. Due to this the lift is no longer only having a non-zero y-component with respect to Figure 2.1. Hence, not the entire lift is used to rotate the blades. However, this effect is very limited for long slender turbine blades.

## 2.2 Momentum theory for an ideal wind turbine

To create a model of a wind turbine it is necessary to know how much energy is extracted from the wind and how the velocity of the wind is decreased passing the rotor. Finding these values can be done by considering an ideal rotor in 1D. An ideal rotor can be considered as a permeable disk that extract kinetic energy of the wind, while being frictionless and adding no rotational energy to the wake.

The wind speed upwind from the rotor, $U_0$ is being slowed down to $U$ at the rotor and $U_i$ downwind from the rotor, due to a drop in pressure over the rotor, $\Delta p$. The pressure upwind from the rotor is atmospheric $p_0$, but increases right before the rotor, drops over the rotor, and continuously goes back to $p_0$ downwind. The pressure drop results in a force slowing down the wind, known as the thrust, $T$. The magnitude of the thrust can be found as:

$$T = \Delta p A \tag{2.1}$$

Where $A$ is the area of the rotor found by $A = \pi R^2$, where $R$ is the radius of the rotor. The flow is assumed to be stationary, frictionless and incompressible. It is further assumed that no external forces act on it neither up- nor downwind of the rotor, hence the Bernoulli equations can be applied. The Bernoulli equation is applied far upwind from the rotor to just before the rotor, where the pressure is $p$:

$$p_0 + \frac{1}{2}\rho U_0^2 = p + \frac{1}{2}\rho U^2 \tag{2.2}$$

where $\rho$ is the density of the air. The Bernoulli equation can also be applied from just downwind of the rotor, where the pressure is $p - \Delta p$ to far downwind:

$$p - \Delta p + \frac{1}{2}\rho U = p_0 + \frac{1}{2}\rho U_i^2 \tag{2.3}$$

Using Eq. (2.2) and (2.3) together gives:

$$\Delta p = \frac{1}{2}\rho \left(U_0^2 - U_i^2\right) \tag{2.4}$$

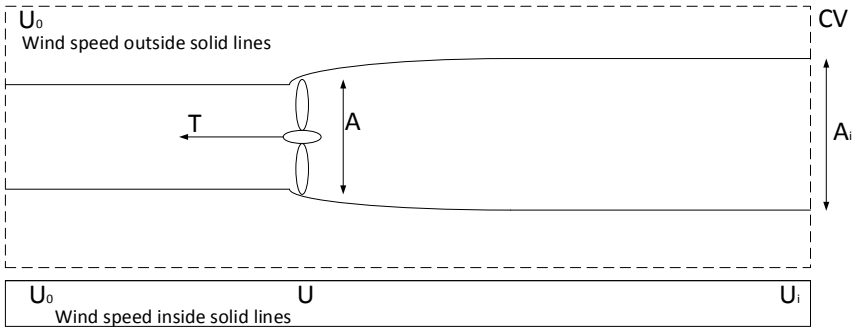


**Figure 2.2:** Definition of control volume (CV) for ideal rotor.

The momentum equation is applied on integral form on the control volume, CV, in Figure 2.2 (marked by the dotted lines) to get an expression for the thrust force. By applying the simplifying assumptions of stationarity, an ideal rotor, and using conservation of mass an expression for the thrust can be obtained. These steps are omitted in this report (for more details see [Han08]) and only the expression for the thrust is presented:

$$T = \rho U A \left(U_0 - U_i\right) \tag{2.5}$$

An expression from the extracted power, $P$, can be extracted by applying the assumption of frictionless flow on the integral power equation on the control volume inside the dotted lines in Figure 2.2. These steps are omitted (see [Han08]) and the expression for the extracted power is:

$$P = \frac{1}{2}\rho U A \left(U_0^2 - U_i^2\right) \tag{2.6}$$

Expressions to calculate $P$ and $T$ have now been obtained. The axial induction factor, $a$, is now introduced as the reduction of the wind speed over the rotor:

$$a = 1 - \frac{U}{U_0} \Leftrightarrow U = \left(1 - a\right) U_0 \tag{2.7}$$

Eq. (2.1) and (2.4) are inserted into Eq. (2.5) to obtain an expression for $T$ and $P$ dependent on $U_0$ and $a$:

$$U = \frac{1}{2}\left(U_0 + U_i\right) \tag{2.8}$$

Using $a$ from Eq. (2.7) gives:

$$U_i = (1-2a)\,U_0 \Leftrightarrow a = \frac{1}{2}\left(1 - \frac{U_i}{U_0}\right) \tag{2.9}$$

It is now possible to rewrite the expression for $P$ using Eq. (2.7) and (2.9):

$$P = \frac{1}{2}\rho\,(1-a)\,AU_0\left(U_0^2 - ((1-2a)\,U_0)^2\right) = 2\rho AU_0^3 a\,(1-a)^2 \tag{2.10}$$

The expression for $T$ is then reformulated:

$$T = 2\rho AU_0^2 a\,(1-a) \tag{2.11}$$

The expressions for $P$ and $T$ are often non-dimensionalised. This is done by scaling $P$ with the total available power in the air, $P_{air}$ given by:

$$P_{air} = \frac{1}{2}\rho AU_0^3 \tag{2.12}$$

Scaling $P$ with the available power gives the power coefficient, $C_P$:

$$C_P = \frac{P}{\frac{1}{2}\rho AU_0^3} = 4a\,(1-a)^2 \tag{2.13}$$

And likewise, $T$ is scaled with the highest possible thrust force, $\frac{1}{2}\rho AU_0^2$, giving, $C_T$:

$$C_T = \frac{T}{\frac{1}{2}\rho AU_0^2} = 4a\,(1-a) \tag{2.14}$$

The power and thrust coefficient will be widely used later. The power coefficient tells how big a percentage of the available kinetic energy in the wind is extracted by the turbine. Given the definition of $C_P$, it is possible to calculate the theoretical maximum limit for the power coefficient for an ideal rotor. Differentiating $C_P$ w.r.t. $a$ gives:

$$\frac{dC_P}{da} = 4\,(1-a)\,(1-3a) \tag{2.15}$$

From this it is easily seen that $C_P$ is obtaining it's maximum at $a = \frac{1}{3}$ (since $a = 1$ gives $CP = 0$). The corresponding maximum $C_p$-value $\frac{16}{27} = 0.5926$. Hence, the theoretical maximal limit of power extraction from the wind given a ideal rotor is 59.26%. This limit is known as the "Betz limit".

## 2.3 Modeling a wind turbine

To analyse the wake effects from wind turbines in a wind farm, a model is needed for describing how the wind flow changes when passing a turbine. The model

| | |
|---|---|
| Rated power | 5 MW |
| Rotor diameter | 126 m |
| Hub height | 90 m |
| Cut-in, Cut-out wind speed | 3 m/s, 25 m/s |
| Cut-in, Rated rotor speed | 6.9 rpm, 12.1 rpm |

**Table 2.1:** Specifications for 5 MW reference turbine

should be able to calculate how much power is produced and how the turbine affects the wind flow as the aim of the project is to optimise the power output for an entire wind farm.

Wind turbines have some limitations that needs to be respected in the model such as cut-in wind speed, cut-in and rated rotor speed, rated power, etc. When building the model these limitations define regions where the turbine is controlled differently depending on the wind speed. The turbine is controlled by changing the angle and rotational speed of the blades. This will be elaborated further in next section.

As different turbines have different specifications a turbine must be chosen for the model. The turbine used in this report is the 5 WM reference turbine (NREL/TP-500-38060), which is described in Jonkman et al. (2009)[JBMS09]. This turbine is chosen since it is widely known in the literature, but also because detailed data for this turbine is available. The specifications affecting the control strategy for the turbine can be seen in Table 2.1. More detailed specifications can be found in Jonkman et al. (2009)[JBMS09]

Before giving a detailed description on how the turbine is controlled two control, parameters must be defined. The first control parameter is the angle of the blades, known as the pitch. The second control parameter is the tip speed ratio, TSR, which describes how fast the tip of the blades is moving compared to the incoming wind speed. TSR is defined as:

$$\lambda = \frac{R\omega}{U_0} \tag{2.16}$$

where $\lambda$ is the TSR, $\omega$ is the rotational speed, and $U_0$ is the wind speed. The power and thrust coefficient for a turbine are dependent on the pitch and the TSR. By changing the pitch and the TSR the turbine can change its power coefficient and produce more or less energy for the same wind speed. The two

coefficients can be defined as functions of pitch and TSR:

$$C_P(\beta, \lambda) \quad C_T(\beta, \lambda) \tag{2.17}$$

where $\beta$ is the pitch. How $C_P$ and $C_T$ are dependent on $\beta$ and $\lambda$ varies from different kind of turbine. The $C_P$- and $C_T$-curves for the reference turbine have been plotted in Figure 2.3. The highest power coefficient is found at $\beta \approx 0$ and $\lambda \approx 7$. The $C_P$-curve has little curvature around the optimum.

The $C_T$-curve has more curvature compared to the $C_P$, meaning that changes in pitch and TSR might affect the thrust coefficient more than the power coefficient.

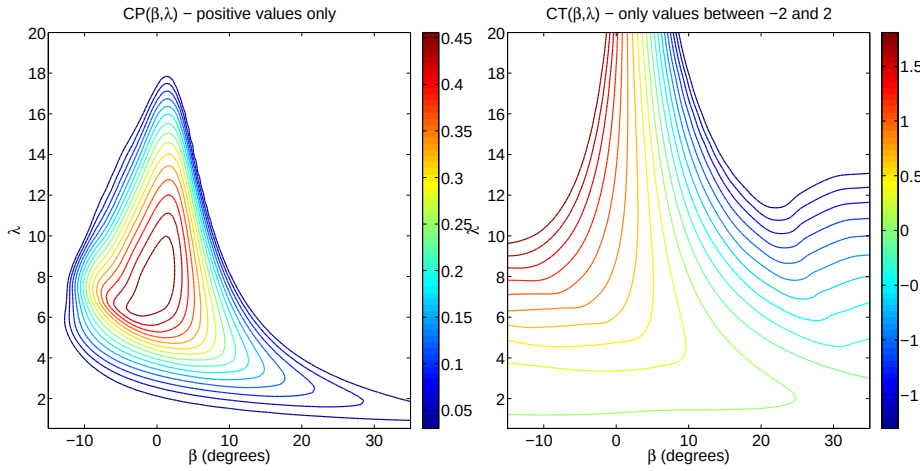


**Figure 2.3:** Plot of the $C_P(\beta, \lambda)$ and $C_T(\beta, \lambda)$, for the 5MW reference turbine. Note, only positive $C_P$ values and $C_T$ values between -2 and 2 are plotted.

### 2.3.1 Control regions

When controlling a turbine the aim is to keep the power coefficient as high as possible, by choosing the best values of TSR and pitch. But due to limitations of the rotor speed and power output, it might not always be possible to choose the optimal $C_P$-value. E.g if the wind speed is above 12 m/s the rated power becomes a constraint and the power coefficient needs to be reduced. Due to the limitations the power curve for the turbine has been split into four regions, the low, mid, high, and top region. In each region different limitations decide how

the optimal power coefficient for that region should be found. Different regions are relevant for different wind speeds. The power curve can be seen at Figure 2.4 together with the rotational speed, thrust coefficient, and power coefficient for different wind speeds.

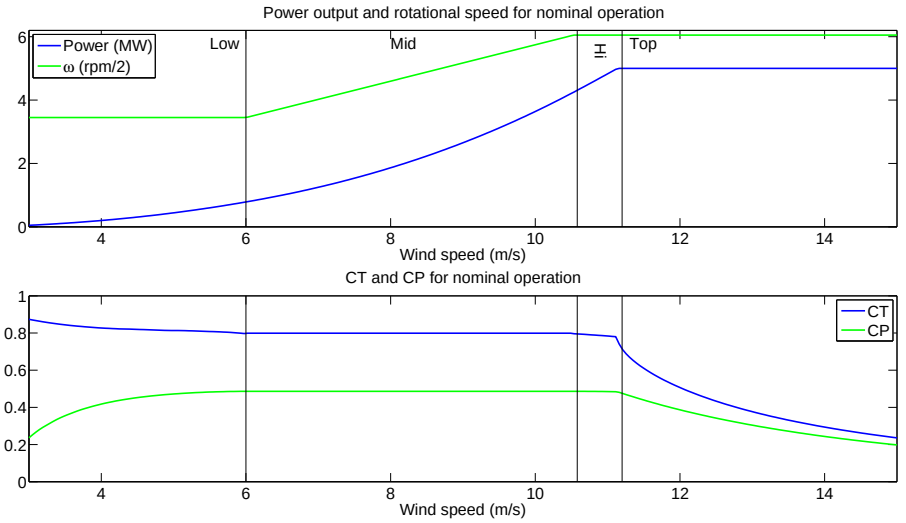


**Figure 2.4:** Top: Power output and rotational speed for the 5MW reference turbine, when running in the nominal case. Bottom: $C_P$ and $C_T$ for the same case.

At top plot in Figure 2.4 the power output and rotational speed are plotted as a function of wind speed, when the turbine is operated in the nominal case, meaning with no down regulation. The rated rational speed is reached before rated power, which is the most common for wind turbine. Also it is noticed that the rotational speed is constant in the low, high and top region, opposite to the mid region where it is increasing linearly for higher wind speeds. In the bottom plot the $C_P$ is seen to be kept constant at its optimal value in the mid region. $C_T$ is high in the first three regions, but decreases fast in the top region. How the turbine is controlled in each region is elaborated in the next four paragraphs.

#### 2.3.1.1 Low Region

The low region starts when the wind speed is higher than the cut-in wind speed. Above this wind speed the turbine can produce power. In the low region the wind speed is so low, that it is not possible to choose the TSR giving the optimal

power coefficient, as this would result in the rotational speed below the cut-in value. Hence, the TSR must then be chosen in such a way that rotational speed is kept at the minimum value. The TSR is set, so that the rotational speed is kept constant in the entire low region in Figure 2.4. The pitch is chosen to maximize the power coefficient for the given TSR, which causes the power coefficient to increase for higher wind speeds. The low region ends when the wind speed is high enough for TSR to be set at the value giving the optimal power coefficient.

#### 2.3.1.2 Mid Region

The mid region starts when the optimal power coefficient can be reached, meaning no limitations on the TSR makes it impossible to run the turbine so that it extracts maximum energy from the wind. In this region the power and thrust coefficient are kept constant, since the pitch and TSR is constant, which also can be seen at Figure 2.4. When the rated rotational speed is reached the TSR must be reduced to ensure that the rotational speed doesn't exceed the rated. At this wind speed the mid region ends and the high region starts.

#### 2.3.1.3 High Region

The optimal power coefficient can't be reached in the high region, since the rated rotational speed is limiting the TSR. The pitch is set to optimize the power coefficient given the reduced TSR. Figure 2.4 shows that the pitch at first is reduced and increased to ensure the best possible power coefficient. The reduction in the power coefficient in the high region is quite small, as the $C_P$-curve have little curvature around its optimum and this region only covers a 1 m/s range of wind speed.

#### 2.3.1.4 Top region

The top region starts when the wind speed is high enough for the turbine to reach full load. Since the power output can't exceed the rated power, the power coefficient has to be reduced. In previous regions where the power coefficient couldn't reach its optimum it was because of a constraint on the TSR but in this region both the pitch and the TSR can be reduced to lower the power coefficient. This introduces a degree of freedom on how to choose the pitch and TSR. The rotational speed has reached its rated speed in this region and cannot be increased further. Keeping the rotational speed at its rated level gives a

unique way of determining the TSR. For a more detailed discussion of other strategies see section 2.3.3. As the turbine is running on full load the power coefficient can be found as $P_{rated}/P_{air}$. A way to find the power coefficient and the TSR has now been defined, meaning that the pitch can be found using the $C_P$-curve. In some cases both a lower and a higher pitch might give the needed power coefficient given the TSR. In these cases the highest pitch is selected, this choice is elaborated in Section 2.3.3.

Together the four regions define how the turbine is controlled given the wind speed in the nominal case. How to down regulate the turbine control is defined in section 2.3.3. In Figure 2.4 it was shown that how $C_P$ and $C_T$ changed for different wind speeds. This was obviously due to changes in the TSR and pitch. On Figure 2.5 the $C_P$- and $C_T$-curves are shown again, together with the pairs of TSR and pitch when running in the nominal setting for wind speeds between 0 to 25 m/s. The left plot shows how the turbine moves on the $C_P$-curve. For lower wind speeds the TSR is high, due to the cut-in rotational speed. As the wind speed increases the turbine moves along the ridge of the $C_P$-curve to the optimal value, this is the low region. In the mid region the $C_P$ is kept constant, since it is also possible to maintain the optimal value. In the high and top regions the $C_P$ value is decreased by decreasing the TSR further and increasing the pitch. When the pitch is increased the $C_T$ value decreases quite fast as it moves toward the lower region of the $C_T$-curve.

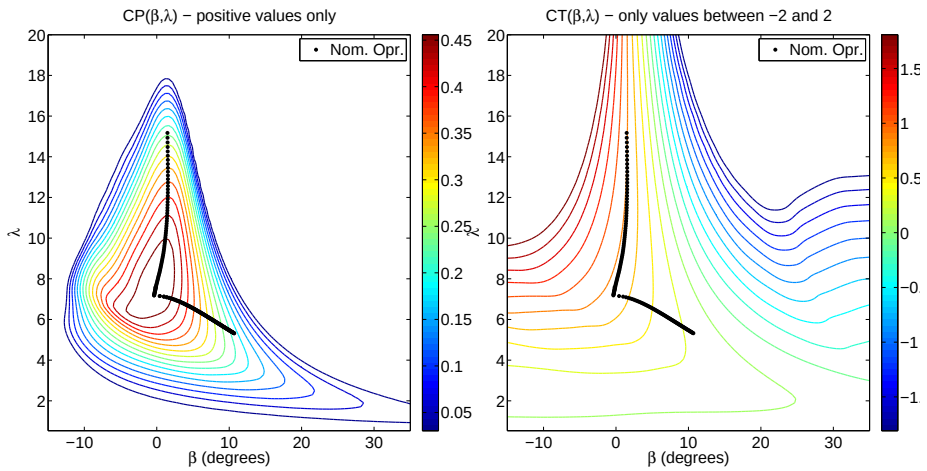


**Figure 2.5:** Relationship between TSR and pitch and the $C_P$- and $C_T$-curves, when running the turbine in nominal setting.

### 2.3.2 Interpolation of the CP- and CT-curves

As mentioned earlier the $C_P$- and $C_T$-curves differ for different turbines and need to be provided to the model. The model needs a $N$x$M$ equidistant grid with values of $C_P$ and $C_T$ together with the $N$ TSR values and $M$ pitch values, where the $C_P$ and $C_T$ are evaluated in (the grid needs to be equidistant in each dimension, the length between points in each dimension can vary). For this report data is given in a 100x100 grid. This means that the data given to the model is not continuous, hence $C_p$ and $C_T$ are only known for $N \cdot M$ points. Pitch and TSR can obviously be chosen continuously, so the $C_P$- and $C_T$-curves need to be interpolated in some way.

There are three cases where the model needs to evaluate the curves for continuous values. The first case is when the TSR and pitch are known and the thrust coefficient needs to be found. The second case is in the high and low region where only the TSR is known due the rotational speed limitations. In this case the pitch must be chosen so that the highest possible value of $C_P$ is achieved given the constraint on TSR. The final case is in the top region, where the power coefficient is limited given the rated power and the TSR is fixed due to rated rotational speed. In this case the pitch should be calculated so that both of the constrains are satisfied.

In the first case where the $C_T$ value is needed given some TSR, $\lambda_0$, and pitch, $\beta_0$ it is unlikely that the $C_T$ is actually evaluated in $(\beta_0, \lambda_0)$, hence the $C_T$-curve needs to be interpolated. To get a smooth interpolation local polynomial regression is used [FG96]. The pitch value closest to $\beta_0$ and the TSR value closest to $\lambda_0$, where $C_T$ is evaluated in, is defined as $(\beta_n, \lambda_m)$. With this point as center, a 9x9 grid of points where $C_T$ is evaluated in is found, meaning 81 points of $C_T$ with corresponding TSR and pitch values are obtained. These 81 points are used to fit a weighted second order polynomial around $(\beta_0, \lambda_0)$. Before the second order polynomial is fitted a kernel function must be chosen to assign weights to 81 points. Since an optimisation algorithm has to be used later on it would be beneficial to choose a kernel function which has continuous derivatives. This is indeed an attribute of the tri-cubic kernel function defined as:

$$W_h(x) = \frac{70}{81}\left(1 - |\frac{x}{h}|^3\right)^3 I\left(|x| < h\right) \tag{2.18}$$

where $I$ is the indicator function and $h$ is bandwidth. As the polynomial is fitted in two dimensions a product kernel is used, i.e:

$$W_{h_\beta, h_\lambda}(\beta - \beta_0, \lambda - \lambda_0) = W_{h_\beta}(\beta - \beta_0) W_{h_\lambda}(\lambda - \lambda_0) \tag{2.19}$$

A bandwidth for both dimensions must be chosen for the kernel function. Since the grid is equidistant in each dimension using the length between evaluated

points is an obvious choice. The maximum distance which any of the 81 points can have to $(\beta_0, \lambda_0)$ is 3.5 times the length between points in each dimension, as the 9x9 grid is centered around the point closest to $(\beta_0, \lambda_0)$. A good choice of the bandwidth is therefore:

$$\begin{aligned} h_\beta &= 3.4\Delta\beta \\ h_\lambda &= 3.4\Delta\lambda \end{aligned} \tag{2.20}$$

where $\Delta\beta = \beta_n - \beta_{n-1}$ and $\Delta\lambda = \lambda_m - \lambda_{m-1}$ is the length between point in the pitch and TSR dimension, respectively. It is now possible to estimate the coefficients of the weighted second order polynomial, since kernel function has been defined. The normal equation is:

$$\hat{\theta} = \left(X^\intercal W\right)^{-1} X^\intercal W Y_{C_T} \tag{2.21}$$

where $\hat{\theta}$ is the coefficients, $Y_{C_T}$ is the $C_T$ values of the 81 points, and $X$ is the design matrix given by:

$$X = \begin{bmatrix} 1 & \beta_1 - \beta_0 & \lambda_1 - \lambda_0 & (\beta_1 - \beta_0)^2 & (\lambda_1 - \lambda_0)^2 & (\beta_1 - \beta_0)(\lambda_1 - \lambda_0) \\ 1 & \beta_2 - \beta_0 & \lambda_2 - \lambda_0 & (\beta_2 - \beta_0)^2 & (\lambda_2 - \lambda_0)^2 & (\beta_2 - \beta_0)(\lambda_2 - \lambda_0) \\ \vdots & \vdots & \vdots & \vdots & \vdots & \vdots \\ 1 & \beta_{81} - \beta_0 & \lambda_{81} - \lambda_0 & (\beta_{81} - \beta_0)^2 & (\lambda_{81} - \lambda_0)^2 & (\beta_{81} - \beta_0)(\lambda_{81} - \lambda_0) \end{bmatrix} \tag{2.22}$$

$\hat{\theta}(1)$ is then the estimated value of $C_T(\beta_0, \lambda_0)$ as the polynomial has been fitted around the point $(\beta_0, \lambda_0)$.

A method to obtain a thrust coefficient given a TSR and a pitch has now been defined. In the second case the pitch needed to be chosen so that is gives the highest possible $C_P$, given a fixed TSR, $\lambda_0$. Since $C_P$ most likely is not evaluated in $\lambda_0$ or the pitch value, $\beta_0$, given the optimal $C_P$, weighted second order polynomial is used to interpolate in a iterative way.

At first the TSR value, $\lambda_m$, closest to $\lambda_0$ where $C_P$ is evaluated is found. Then the pitch value, $\beta_n$, where $C_P$ is evaluated in giving the the highest $C_P$ for $\lambda_m$ is found. A 9x9 grid centered around $(\beta_n, \lambda_m)$ is used to find $\hat{\theta}$, the same way as before, by fitting the second order polynomial around $(\beta_m, \lambda_0)$. When keeping $\lambda_0$ fixed the optimum of $C_P(\beta^*, \lambda_0)$ only depends on $\beta^*$. This value can be found by optimising the second order polynomial of $C_P(\beta^*, \lambda_0)$ and can be done analytically. When a value of $\beta^*$ has been found a new second order polynomial is fitted around $(\beta^*, \lambda_0)$ for the same 9x9 grid. A new estimate of the optimal pitch, $\beta^*$, can then be obtained. This iterative method is used until the change in $\beta^*$ for each iteration is smaller than 0.01. When the change in $\beta^*$ is smaller than the threshold the iterations stops. The pitch, $\beta_0$, giving the highest $C_P$ for $\lambda_0$ has now been found, and $C_P(\beta_0, \lambda_0)$ is then found in the same way as $C_T(\beta_0, \lambda_0)$ was found.

The final case where the curves need to be evaluated continuously is when a pitch must be found given a fixed power coefficient, $C_{P0}$, and a fixed TSR, $\lambda_0$, which indeed is the case in the high region. Once again weighted second order polynomials are used to interpolate in a iterative way. The setup is very similar to the previous case, except finding $\beta^*$ is done by solving the second order polynomial, instead of finding the pitch optimising $C_P$. As this include solving a second order polynomial two solutions for $\beta^*$ might be found. As mentioned in section 2.3.1 the highest pitch is always chosen, for reasons given in section 2.3.3.

When solving the second order polynomial the discriminant might sometimes be negative, meaning it is not possible to reach $C_{P0}$ for the given second order polynomial. This happens because the second order polynomials are only an approximation of the $C_P$-curve and the approximation is fitted around a point too far from the real solution. This causes the two pitch values solving the problem to be complex. The two solutions has the same real part, which is the pitch optimising the second order polynomial. As the $C_{P0}$ can't be reached $\beta^*$ is chosen as the real part of the solutions, since this gives the highest $C_P$ and thereby the $C_P$ closest to $C_{P0}$ for the current second order polynomial. A new second order polynomial is then fitted around the updated $(\beta^*, \lambda_0)$. The updated $\beta^*$ is closer to the pitch, $\beta_0$, giving $C_{P0}$ for $\lambda_0$ and complex solutions of the problem are less likely to occur. When $\beta^*$ is sufficient close to $\beta_0$ the second order polynomial fit the $C_P$-curve well and complex solutions won't occur.

Methods for evaluating the $C_P$- and $C_T$-curves for continuous input has now been defined. Since weighted second other polynomials has been used, jumps should not occur as the interpolation method used is sufficient smooth.

### 2.3.3 Down regulation of the turbine

In this report down regulation of turbines is used to increase the total power production for entire wind farms by curtailing upwind turbine. A gain in the total power production can be achieved when the loss of power from down regulating upwind turbines is smaller than the gain in power from the increased wind at the downwind turbines. E.g consider two turbines, A and B, where the B is in full wake of turbine A. If turbine A is down regulated 0.5 MW and thereby leaving more energy in the wind for turbine B. Then the gain turbine B might be bigger than 0.5 MW and the total power production of the two turbines is increased.

So far a control strategy for the turbine has only been defined for running in the nominal case. The aim of this report is to analyse whether a gain might be

achieved by curtailing upwind turbines. To do so a strategy for down regulation of turbines must to be defined.

Down regulation of a turbine is done when the demanded power, $P_d$, of the turbine is smaller than what is obtainable in nominal operation, $P_n(U_0)$, for a given wind speed, $U_0$. $P_d$ can be reached at wind speed $U_d$, which is lower than $U_0$. Making a turbine produce less power is done by not choosing the highest possible power coefficient but choosing a power coefficient equal to $\frac{P_d}{P_{air}}$. Lowering the power coefficient meaning descending to a lower level on the $C_P$-curve. Going to a lower level on the $C_P$-curve introduces a degree of freedom as both the pitch and TSR can be adjusted to give the needed power coefficient. Some restrictions on the TSR are of course still present, as the limitations on the rotational speed should be meet. The down regulation strategy is a definition of how to choose the TSR and pitch for reduced power coefficients.

In Mirzaei et al. (2014)[MSPN14] three different strategies for down regulation is defined. The first strategy is to maximise the rotational speed. This means, that the power coefficient is reduced by increasing the rotational speed as much as possible. The rotational speed can be increased until the demanded power coefficient can't be reached for higher values of TSR or until the rated rotational speed is reached. By maximising the rotational speed a unique way of determining the TSR is defined. The second strategy is to keep the rotational constant compared to the speed found for nominal operation for wind speed $U_d$. As the rotational speed is kept at the same speed for all wind speeds higher than $U_d$, a unique way of finding the TSR is defined. When the TSR is known the pitch can be found, as the power coefficient is also known when down regulating. The third strategy is to keep the TSR constant. This can be done until the rated rotational speed is reached, after this point the rotational speed is kept at its rated. This strategy once again gives a unique way to determine the TSR.

In the two last strategies two pitches might give the needed power coefficient for a fixed TSR. The smallest of the two pitches is said to be in the stall region. It is preferred to operate the turbine away from the stall region, which is why the higher pitch angle is used in this report.

A comparison of the three strategies is done in Mirzaei (2014)[MSPN14]. The constant TSR strategy is suggested, since it is combining favorable features from the maximum and constant rotational speed strategies. The favorable features are among other thing related to smooth transition in rotational speed for changing wind speed and operation away from the stall region. For details more details see [MSPN14]. As the constant TSR strategy is suggested this down regulation strategy is used in this report.

Chapter 3

# Wake effects from wind turbines

As mentioned wind turbines extract kinetic energy from the wind that passes through the rotor. The wind field behind a turbine with an decreased kinetic energy is called the wake. Modeling wake effects from wind turbines is considered difficult as it involves describing the aerodynamics of a unsteady complex system in which some issues are not yet fully described and quantified [VSC03]. The wake of wind turbines is also affected by the atmospheric conditions in which the turbine is located. The most important atmospheric conditions are introduced in this chapter followed by a brief description of different ways to model wake effects. Finally, a more detailed description of the model used for this report is presented.

## 3.1 Atmospheric conditions

In this section the most important atmospheric conditions affecting the wake are introduced. The purpose is to give framework for understanding the different approaches for wake modeling that will be presented later in this chapter. The paper by Sandersee (2009) [San09] is used repeatedly in this section and will not be referred to continuously.

#### 3.1.0.1 Surface roughness length

The surface of the ground is affecting the wind field above it, as wind flows more undisturbed across a flat terrain than across a forest or an urban area. The surface roughness length is a number related to the height of the elements on the ground surface. The surface roughness length will be larger for uneven surfaces e.g. it is 0.001 meters rough sea and 0.03 meters for open flat terrain. One of the first ways to model wakes was by changing the surface roughness around turbines [New77]. The recovery of velocity and expansion of the wake is smaller off-shore than on-shore, as the surface roughness length off-shore are considerably smaller.

#### 3.1.0.2 Atmospheric boundary layer

The atmospheric boundary layer (ABL), also known as planetary boundary layer, is the lowest part of the atmosphere where the wind is influenced by the surface roughness. Above this layer the wind is considered not to be affected by the surface and usually to be non-turbulent. When the wind is affected by the surface velocity components not parallel to the mean wind flow are introduced. This affects the turbulence of the wind and makes the wind field more unsteady. The velocity of the wind is increasing in the ABL as the height above ground increases and is often modeled by a logarithmic approximation dependent on the surface roughness length. The layer starts at the ground surface and for different surfaces reaches from a hundred meters to a few kilometers in height.

#### 3.1.0.3 Atmospheric Stability

The atmospheric stability is telling if the air rising from the surface is in thermal equilibrium with the surrounding air, in that case the stratification is said to be neutral. Neutral stratification is typically met during strong winds and in the afternoon. If the stratification is unstable the turbulence in the air is caused by large-scale eddies and the ABL is thick. This is often the case during daytime. When the stratification is stable, typically during night and in low winds, the surface roughness is the main cause to turbulence and the ABL to be thin.

#### 3.1.0.4 Turbulence

Atmospheric turbulence is occurring in the ABL because the surface roughness is causing disturbance in the wind flow. An unstable stratification causes increased turbulence as large-scale eddies rise from the surface. Rotor induced turbulence is introduced when the wind meets a rotor as deviations are introduced in the wind velocity because of vortexes from the blade-tips. The turbulence intensity, which is often used in wake models, is defined as:

$$I_{\bar{U}} = \frac{\sigma_{\bar{U}}}{\hat{U}} \tag{3.1}$$

where $\bar{U}$ is the average wind velocity, and $\sigma_{\bar{U}}$ is the standard deviation in the average wind velocity. As the wind field in wakes have passed a rotor they are considered to be more turbulent than the free wind field. Higher turbulence causes wind flows to mix faster with the free wind flow and is also related to increased loadings on turbines.

## 3.2 Modeling of wakes

Wakes are usually studied in two regions with different characteristics, namely the near and the far wake. The near wake starts from just downwind of the rotor and extend to 2 to 5 rotor diameters downwind [CHF99]. The wake in this region is characterised by steep pressure gradients and blade tip vortexes. The vortexes cause a layer of turbulent air between the wake and the free wind. The mixing of the wake and the free wind are not the same above and below the wake, causing the recovery and expansion to be different above and below the wake. The increased turbulence works as an efficient mixer, where the high velocity free wind mixes with low velocity wake [San09]. In the near wake the wake is expanding and recovering more and faster than in the far wake.

The far wake is no longer characterised by vortexes and pressure gradients and is not expanding or recovering the wake deficit as much as in the near wake. In this region the atmospheric turbulence is the main reason for expansion and recovery, meaning that stable stratification and surface roughness affect the recovery. A self-similar and axisymmetric velocity deficit profile is often assumed in this region, as the pressure gradients are less influential and often neglected. The far wake region is the one of most interest when working with optimising set points distribution in off-shore wind farm as the distance between turbines often is sufficiently large.

## 3.3 Wake models

Several motivations for modeling wakes exist e.g. analysing loadings on turbines, evaluating wind farm controllers or calculating wind farm efficiencies. Different purposes require more or less accurate models including various features. The models in this report are categorised into two categories, namely kinematic and field models.

### 3.3.1 Kinematic models

The kinematic wake models are the simplest category of wake models described in this report and does in general not require much computational capacity. They are normally based on an assumption of a self-similar and axisymmetric velocity deficit profile, which is assumed only in the far wake. In almost all of the models the velocity deficit is calculated using the global momentum equation, using the thrust coefficient from upwind turbines [VSC03]. Assuming self-similarity and axisymmetric causes it difficult for the models to handle interactions with the ground and the ambient wind shear. Even though the kinematics uses unrealistic assumptions they have proven to be in good agreement with experiments and giving a reasonable estimate of wake losses in wind farms [CHF99]. The loadings on the turbines cannot be calculated with these models. In general these models are used for controlling wind farms where fast models are needed.

One of the most commonly used kinematic models is developed by Jensen (1983)[Jen83], assuming an (axisymmetric) "top-hat"-shaped velocity deficit profile that expands linearly. This model is widely known for its simplicity and robustness. This model is used for calculating wake deficits in this report and a more detailed description is given later.

A more recent model is the semi-analytical model by Larsen (2009) [Lar09], based on solving the Navier-Stokes equations for experimental data. This model also assumes axisymmetric velocity and turbulence profiles and a non-linear wake expansion profile. The turbulence intensity is included in this model, but the improvement is shown to be limited compared to the Jensen wake model [GRB+12]. However, the model is expected to estimates the the wake deficits better for larger wind farms, as the Jensen model is considering to over estimate the wake deficit for large wind farms[CC13].

### 3.3.2 Field models

The field models separate themselves from the kinematic model by describing every point of the entire flow field behind a turbine. This type of model is usually more complex, but allows to describe more phenomenons in the wake and to account for effect of more ambient conditions. Most of these model solve the Reynolds-averaged Navier-stokes equations (RANS) [CHF99], with more or less simplifying assumption. Ainslie (1988) [Ain88] is known for the Eddy Viscosity model which is very common in the literature. The model solving the RANS in cylindrical coordinates, neglecting pressure gradients outside the wake and assuming Gaussian velocity deficit profile. This model considers ambient turbulence as main contribution to mixing of the wake and ambient flow. Interactions with the ground and varying wind velocities in the ABL with height are not included. The slightly more advance model UPMWAKE considers velocity changes in the ABL and also atmospheric stability. This model shows that the wake deficit is larger below rotor height than above for neutral and stable stratification with small surface roughness and little turbulence.

Complex models without the simplifying assumptions used in Ainslie (1988)[Ain88] have also been developed. These models give a more accurate and detailed description of the wake, including the near wake. The computational needs for these models are larger but still have issues handling time-varying thermal structures in the ABL and large pressure gradients [BRBA12]. An alternative method for detailed description of wakes is the large eddy simulations (LES). These models are couple with an actuator disk/line model (see [San09] for details on the actuator disk concept) and gives very good results compared to experiments even in the near wake. However, these models are very computational demanding and require high performance computers.

The field models can be used to describe the more complex phenomenons of the wake and describe the near wake in details which the kinematic models aren't able to handle. The field models provides more detailed information about the wakes. Their results are used for purposes where more accurate models are required, for example for optimising wind farm layouts, validating performance of control strategies or verifying results of simpler models [ASJ+14]. E.g. LES was used to validate a new approach on wake modeling, namely using a particle filter to track the wake locations [FGC+14].

## 3.4 Jensen wake model

The model used in the report is the Jensen's wake model [Jen83]. As mentioned the model is quite simple but known for good performance. Since the model should be used for controlling it should be sufficiently fast. Another candidate was the Larsen model which in Crasto (2013) [CC13] showed less overestimation of the wakes for downwind turbines when narrow bins of wind direction were analysed. However, other comparisons of the two models have shown little difference in performance, which is why the simple Jensen model is used.

The Jensen model is based on the balance of momentum equation, and assuming a linear expansion with slope $\alpha$ and constant axial speed in the entire wake, giving a "top-hat" shaped wake profile. $\alpha$ is known as the wake decay constant and depends on the ambient conditions. The coefficient is high when the wake spread faster, meaning the wake recover over a short distance. Atmospheric stability, changing in-flow velocity in with respect to height in the ABL, ambient turbulence and surface roughness are not directly included in this model but by changing the wake decay constant the recovery of the wake can be controlled. For off-shore wind farms a decay constant of 0.04 is usually used [BRBA12, MBG+14], the same constant will be used in this report. The model is only valid in the far wake where the rotor induced turbulence and pressure gradient are assumed negligible.

A control volume has been defined in Figure 3.1. Using the notation from the figure and applying conservation of mass just downwind of the rotor and further downwind where the diameter of the wake is $D_w$ gives:

$$\pi \left(\frac{D}{2}\right)^2 U_r + \pi \left(\left(\frac{D_w}{2}\right)^2 - \left(\frac{D}{2}\right)^2\right) U_0 = \pi \left(\frac{D_w}{2}\right)^2 U_w \tag{3.2}$$

As the wake expand linearly with slope $\alpha$ the diameter downwind of the wake can be calculated as:

$$D_w = D + 2\alpha\Delta x \tag{3.3}$$

where $\Delta x$ is the distance downwind. Combining Eq. (3.2) and (3.3) gives the definition of the velocity deficit:

$$\Delta U = 1 - \frac{U_w}{U_0} = \frac{2(1 - \frac{U_r}{U_0})}{(1 + \frac{2\alpha\Delta x}{D})^2} \tag{3.4}$$

Using the definition of the axial induction, $a = \frac{1}{2}\left(1 - \frac{U_r}{U_0}\right)$, from Eq. (2.9)

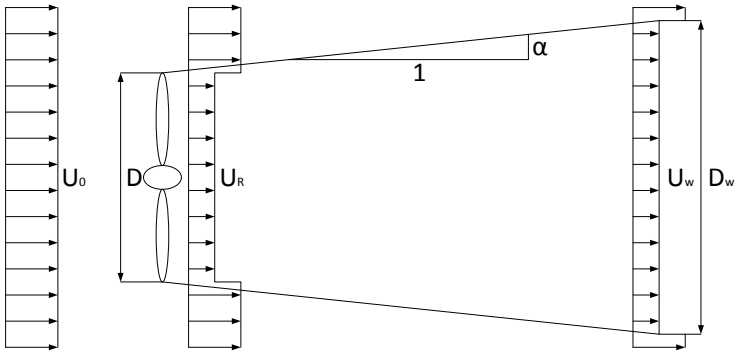


**Figure 3.1:** Definition of control volume used for Jensen's wake model.

gives:

$$\Delta U = \frac{2a}{(1 + \frac{2\alpha\Delta x}{D})^2} \tag{3.5}$$

Solving the trust coefficient from Eq. () for the axial induction factor gives:

$$a = \frac{1 - \sqrt{C_T}}{2} \tag{3.6}$$

Inserting Eq. (3.6) into (3.5)

$$\Delta U = \frac{1 - \sqrt{1 - C_T}}{(1 + \frac{2\alpha\Delta x}{D})^2} \tag{3.7}$$

It is now possible to calculate the wind speed in the wake further downwind using the velocity deficit from (3.7) and the thrust coefficient from the upwind turbine.

### 3.4.1 Partial wake

The expression from (3.7) only gives the wind speed inside the wake. A wake from an upwind turbine might only affect a downwind turbine partially, meaning not the entire rotor of the downwind turbine is in wake. On Figure 3.2 the situations of full wake and partial wake are illustrated. $A_w$ is the area of the wake at some downwind distance, when the wake radius has expanded to $R_w$. $R$ is the rotor radius for the $i$'th downwind turbine, and $A_{j,i}$ is the area where the wake of the $j$'th turbine overlaps the $i$'th rotor. $D_{j,i}$ is the cross-wind distance between turbine $i$ and $j$, and is defined as the distance between the turbine perpendicular to the direction of the wind. The cross-wind distance can be used

to calculate if the downwind turbine is in full wake, partial wake or not in wake at all.

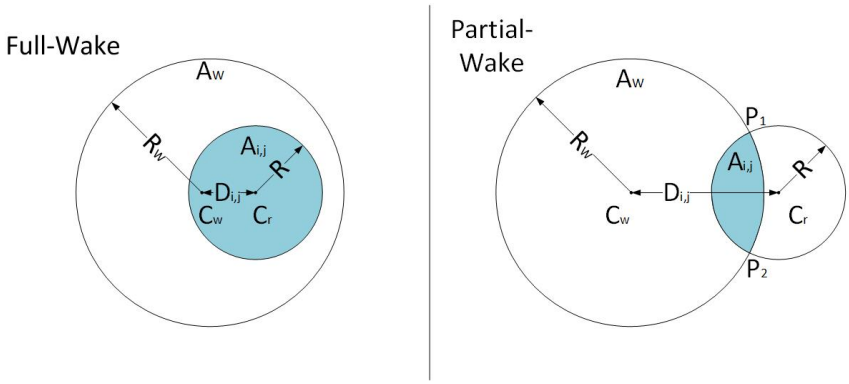


**Figure 3.2:** Illustration of full wake and partial wake. Full wake happens when $D_{j,i} \leq R_w + R$ and partial wake when $R_w - R \leq D_{i,j} \leq R_w + R$.

On Figure 3.2 in the case of the full wake it is easy to see that the wind speed at the $i$'th should be the wind speed inside the wake. In the case with partial wake the entire rotor is not affected by the wake and the wake deficit cannot be calculated that simple. In this case the velocity deficit can, according to Wan (2012) [WWY+12], be calculated as:

$$\Delta U_{j,i} = \Delta \tilde{U_{j,i}} q_{i,j} \tag{3.8}$$

where $\Delta \tilde{U_{j,i}}$ is the velocity deficit inside the wake from turbine $j$ at the downwind turbine $i$. $\Delta U_{j,i}$ is velocity deficit at the $i$'th turbine from the $j$'th turbines wake corrected for partial wake conditions and $q_{j,i}$ is the percentage of the downwind rotor covered by the wake, define by:

$$q_{j,i} = \frac{A_{j,i}}{A} \tag{3.9}$$

where $A$ is the area of the rotor. $A_{j,i}$ can be found be:

$$A_{j,i} = \begin{cases} \pi R^2 & \text{for } D_{j,i} \leq R_w + R \\ \frac{1}{2}R^2\left(\alpha_1 - \sin(\alpha_1)\right) + \frac{1}{2}R_w^2\left(\alpha_2 - \sin(\alpha_2)\right) & \text{for } R_w - R \leq D_{j,i} \leq R_w + R \\ 0 & \text{for } R_w - R \leq D_{j,i} \end{cases} \tag{3.10}$$

where $\alpha_1$ and $\alpha_2$ are defined as:

$$\alpha_1 \triangleq \angle P_1 C_w P_2 = 2 \arccos\left(\frac{R^2 + D_{i,j}^2 - R_w^2}{2RD_{i,j}}\right) \tag{3.11}$$

$$\alpha_2 \triangleq \angle P_1 C_r P_2 = 2 \arccos\left(\frac{R_w^2 + D_{i,j}^2 - R^2}{2R_w D_{i,j}}\right) \tag{3.12}$$

where $C_w$ and $C_r$ is the center of wake the downwind rotor, respectively, and $P_1$ and $P_2$ are points defined on Figure 3.2. Being able to model the partly wake situations is important as the Jensen model assumes a "top-hat" wake shape. If there were no partial wake region the wind speeds in front of a turbines in wake would jump when the wind direction changes just a bit.

### 3.4.2 Wake superposition

The Jensen wake model has been defined for wake interaction between turbines in the case of partial and full wake. No method for handling multiple wakes on one turbine has been defined yet. Different methods to handle multiple wakes exist where the two most common are linear and quadratic superposition. In Katic (1986) [KHJ86] the quadratic superposition is proposed for the Jensen model and is also the most common for the Jensen model as well [CC13, GRB+12]. However, the linear superposition is also seen but have a tendency of leading to negative velocities when many wakes affect the same turbine [CHF99].

The quadratic superposition is used in this report, meaning the wake deficit at a downwind turbine is calculated as the square root of the squared sums of wake deficits from all upwind turbine. Hence, the wind speed in front of turbine $i$ can be calculated as:

$$U_i = U_0 \left(1 - \sqrt{\sum_{i=1}^{N} \left(\Delta U_{i,j}\right)^2}\right) \tag{3.13}$$

where $N$ is the number of turbines in the farm and $U_i$ is wind speed in front of turbine $i$. The wind speed reduction for downwind turbines has been analysed for a row of seven turbines standing in full wake of each other with five rotor diameter distance. The normalised wind speed in front of each turbine has been plotted in Figure 3.3 using the Jensen wake model with both the quadratic and linear wake deficit superposition. Turbines are in nominal operation.

At Figure 3.3 it shows that the wind speed decreases for turbines further downwind which is as expected. For the quadratic superposition the wind speeds seem to reach an equilibrium around Turbine 3, meaning that the wind speed

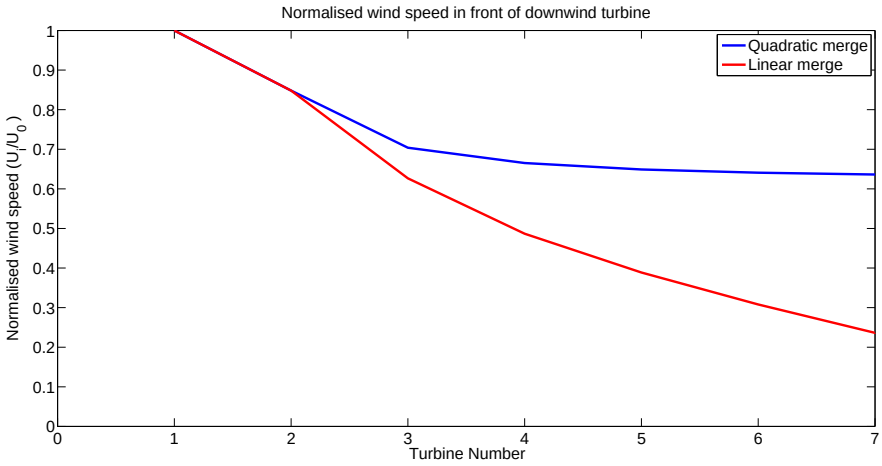


**Figure 3.3:** Plot of the normalised wind speed in front of each turbine for a row of seven turbines, using both the quadratic and linear wake superposition.

in front of turbines further downstream of Turbine 3 is almost the same. This property is not seen for the linear superposition, as it keeps decreasing and doesn't reach an equilibrium.

Experiments show that the wind speed indeed reaches a equilibrium around the third or forth downwind turbine [CC13, BRBA12, CHF99]. This confirms that the quadratic superposition gives the most realistic results for the Jensen wake model. A method for calculating the wind speed in front of a turbine has now been defined both for situations where multiple wakes and partial wakes affect a turbine.

Chapter 4

# Optimizing set point distributions for row wind farms

The purpose of this report is to investigate if it is possible to increase the total power production for wind farms by curtailing upwind turbines. The turbine model from Chapter 2 gave information about a single turbine only. In the previous chapter it was described how the turbines interact with each other through wake effects and a model for calculating the velocity deficits was formulated. Before it is possible to calculate the total power production of a wind farm these two models must be combined.

The most commonly used strategy for optimising wind farms is to use maximum power point tracking (MPPT). This means that the turbines are optimised individually to extract as much power from wind the as possible, without considering the consequences of the wake effects. I.e. losses to wake effects are just accepted and nothing is done to prevent them. MPPT will be compared with a strategy where upwind turbines will be curtailed to improve the power production for wind farms. Other methods of optimising wind farms are also seen, e.g by yawing (turning direction of the wake) the wake so downwind turbines are less exposed to wake effects [GTvW+14].

The turbine model and the wake model are dependent on each other. The wake model needs the thrust coefficient to calculate the wind speed in front of downwind turbines. On the other hand, the thrust coefficient is given as an output from the turbine model. Hence, before being able to calculate the wind speed in front of a turbine it must be known if the turbine is in the wake of an other turbine.

Wake effects in wind farms obviously depends on the layout of the farm and the direction of the wind. In this report a stationary wind flow is assumed, meaning that the free wind speed and wind direction is known and constant over time. Using this assumption and Jensen's wake model makes it possible to calculate which turbines are in the wake of each other, given a wind farm layout and a wind direction.

## 4.1 Formulation of optimisation problem

The available power for each turbine can be calculated iteratively when it is known which turbines are in the wake of each other. The available power on a downstream turbine can be decided when the wake deficit from all upwind turbines is known. By calculating the wake deficit from the most upwind turbines first (this turbine is always in free wind), it is possible to calculate the available power on all turbines in a wind farm.

Set points must be provided to the turbine model as it allows for down regulation. It was shown in Chapter 2 that the thrust coefficient was affected when the turbine was down regulated. Hence, when the set points of an upwind turbine is reduced, the wake deficit will be smaller for all downwind turbines. Finding the distribution of set points that maximises total power production of the farm can be formulated as an optimisation problem.

The total power production from the wind farm should be maximised given a wind farm layout, a free wind speed, and the wind direction. Hence, the optmimal distribution of set points can be found as:

$$\max_{x_i \text{ for } i \in I} \quad P(\mathbf{x}, U_0) = \sum_{i \in I} p(x_i, U_i) \tag{4.1}$$

$x_i$ is the set point for turbine $i$, $\mathbf{x}$ is a vector containing the set points for turbine $i \in I$, where $I = \{1, 2, ..., N\}$, and $N$ is the number of turbines in the wind farm. $U_0$ is the free wind speed and $U_i$ is the wind speed just in front of turbine $i$. $p(x_i, U_i)$ is the power production on turbine $i$ given the set point and the wind speed just in front the turbine. If the set point is higher than the available

power on the turbine given the wind speed, $p(x_i, U_i)$ is equal to the available power.

The problem consist of optimising $N$ variables as the set point for each turbine should be optimised. It would be beneficial to reduce the size of the problem, since larger problems are more difficult and take longer to solve. When optimising turbines with no turbines in its wake the best solution is always to extract as much power as possible. This means that only turbines with another turbine in its wake should have their set point optimised. The optimisation problem can then be reduced to:

$$\max_{x_i \text{ for } i \in J} \quad P(\mathbf{x}, U_0) = \sum_{i \in I} p(x_i, U_i) \tag{4.2}$$

where $J$ is the subset of $I$ consisting of all turbines having at least one turbine in its wake. The set of turbines $I \setminus J$ is always run in nominal operation as no gain can come from down regulating turbines with no turbines in their wake. The optimisation problem is solved by applying MATLAB's gradient based unconstrained numerical solver `fminunc()`. The algorithm uses a Quasi-Newton finite-difference method to approximate the hessian, as the gradient of the objective function is unknown.

## 4.2 Analysing optimisation problem

Finding the optimal set point distribution has now been formulated as an optimisation problem. To validate the defined method for solving the optimisation problem a very small wind farm is analysed. A simple wind farm to analyse is a row wind farm consisting of only 2 turbines, where the first turbine is in full wake of the other. Turbine 2 is the turbine in full wake of Turbine 1 and is placed 5 rotor diameters (630m) downstream in the direction of the wind. Only the set point of Turbine 1 needs to be optimised as Turbine 2 has no turbines in its wake. As only one set point should be optimised the problem is considered simple to solve.

Before using the solver to solve the problem a few challenges will be considered. The first challenge is that `fminunc()` solves unconstrained problems, meaning that the turbine model should be able to take all real numbers as an input. The second challenge is that the `fminunc()` is gradient based, so the objective function should have curvature everywhere. The final challenge is that the objective function has more global optimums in in some cases. E.g. when the wind speed is low so that if Turbine 1 is started the wind speed in front of Turbine 2 is below the cut-in speed. This case has more optimums as is doesn't

matter which one of the turbines is started since the total power production would be the same.

The turbine model should give meaningful power output, no matter what real number it is given as set point. The model should handle negative set points and set points higher than the available power on the turbine. As mentioned before the turbine model returns the highest available power when the given set point is higher than the available power. If a negative set point is provided to the model it will always return 0. This introduces an issue with the objective function not having curvature everywhere. This issue arises when unreachable set points are given to the model. The turbine model gives the same output for all negative set points and for all set points higher than the available power, which causes the objective function to be constant for those set points. To solve the issues with no curvature and more global maximums, when not all turbines are started, penalty functions are added to the objective function.

### 4.2.1 Penalty functions

Adding penalty functions to the objective function can solve the above mentioned issues, so that the optimisation algorithm can be applied. Two penalty functions are defined, one to solve the challenge with no curvature for unreachable set points and one to avoid several optimal solutions when not all turbines are started.

The penalty added for providing unreachable set points to the turbine model should depend on how far the given set point is from a reachable set point. A new variable $\delta_i$ is defined as distance from an unreachable set point to the closets reachable set point for turbine $i$, i.e:

$$\delta_i = \begin{cases} -x_i & \text{for } x_i < 0 \\ x_i - p(x_i, U_i) & \text{for } x_i > p(x_i, U_i) \\ 0 & \text{otherwise} \end{cases} \tag{4.3}$$

The used solver is gradient based and therefore the penalty function should preferably be continuous and have continuous derivatives. To ensure this a piece-wise penalty function is defined with $\delta_i$ as input. For set points with a small $\delta_i$ a quadratic penalty function is used and for set points with a larger $\delta_i$ a linear penalty function is used. The penalty function should be defined so that it has the same gradient and same penalty for both the linear and quadratic penalty in the point where it changes from being quadratic to linear, to ensure continuous derivatives. The gradient should also go towards 0 as $\delta_i$ goes to 0 to give continuous derivatives around $\delta_i = 0$. A penalty function, $\Phi_1(\delta_i)$, is

defined:

$$\Phi_1(\delta_i) = \begin{cases} \phi_1 \delta_i^2 & \text{for } \delta_i < \phi_2 \\ 2\phi_1\phi_2\delta_i - \phi_1\phi_2^2 & \text{for } \delta_i > \phi_2 \end{cases} \tag{4.4}$$

where $\phi_1$ is the penalty factor (how hard unreachable set points are penalised) and $\phi_2$ is the point when the penalty function goes from being quadratic to linear. $\Phi_1(\delta_i)$ is seen to be continuous and has continuous derivatives and is used as penalty in the objective function.

To avoid more global optimums when not all turbines are started a second penalty function is defined. Considering the row wind farm with two turbines, when there is only enough wind to have one turbine running. If the wind speed increases the second turbine needs to be started at some point. It will be shown later that when the second turbine is started the total power production is highest when Turbine 1 produces the most power. Hence, in the case with not enough wind for having both turbines running, it will always be beneficial to start Turbine 1 first, since this turbine should produce the most power. If Turbine 2 was started first, this turbine would have to be down regulated and Turbine 1 would have to be started at a higher load.

A solution to the problem with more global maximums on the objective function is to add a penalty if a turbine produces less power than turbines in its wake. This penalty works for larger wind farms with many turbines, since it should always be optimal to start the upwind turbines first. To define this penalty as a function it is necessary to know which turbines stand in the wake of other turbines. A new set $W_i$ is defined for each turbine to keep track of which turbines stand in the wake of turbine $i$. E.g for the row wind farm with two turbines $W_1 = \{2\}$ and $W_2 = \emptyset$.

The penalty should be dependent on how much more power downwind turbines produces compared to their upwind turbines. A new variable $\Delta T_{i,j}$ is defined as the amount of power turbine $j$ produces more than turbine $i$:

$$\Delta T_{i,j} = \max(p(x_j, U_j) - p(x_i, U_i), 0) \tag{4.5}$$

The second penalty function should have the same attributes as $\Phi_1(\delta)$ with respect to continuity. The penalty added to the objective function, for having a turbine producing less power than a turbine in its wake, should be larger than difference in power production for the two turbines. The second penalty function, $\Phi_2(W_i)$, is defined:

$$\Phi_2(W_i) = \sum_{j \in W_i} \Delta T_{i,j} + \Phi_1(\Delta T_{i,j}) \tag{4.6}$$

The first element in the penalty function $\Delta T_{i,j}$ ensures that the objective function can never be increased by letting a downwind turbine produce more power

than its upwind turbines. The second element $\Phi_1(\Delta T_{i,j})$ adds a penalty (which meets the continuity requirements) to the objective function and it is decreased when a downwind turbine produces less power than its upwind turbines.

A new objective function which doesn't have the issues with no curvature and more global optimums can now be defined by using the two penalty functions:

$$\max_{x_i \text{ for } i \in J} \quad P(\mathbf{x}, U_0) = \sum_{i \in I} (p(x_i, U_i) - \Phi_2(W_i)) - \sum_{i \in J} \Phi_1(\delta_i) \tag{4.7}$$

Two comments about the new objective function should be noticed. The penalty function $\Phi_1$ is only applied on turbines which have their set points optimised, as the set points for turbines with no turbine in their wake are always the rated power. The second comment is that by introducing the second penalty function $\Phi_2(W_i)$ the true global maximum is in fact changed in some cases. Consider three turbines on a row where the wind direction is head on, so that the last turbine is in full wake of the middle, and first turbine and the middle turbine is in full wake of the first. If the wind speed is so low that only two turbines can be running the new objective functions maximum is to have the first and middle turbine running. However, the true optimal setting is to have the first and last turbine running as the wind would recover more over the longer distance. When working with larger wind farms many cases like could be considered.

This issue is not solved in this report, but it is only affecting results for low wind speeds. The difference in total power output is assumed to be quite small. However, a big gain from using the defined objective function is that the optimal set point distribution should not change much when the wind speed is only changed a bit. If it was allowed to start turbines further downwind in a wind farm these turbines would at some point be shut down to start turbine upwind instead when the wind increases. This causes the optimal set point distribution to change a lot (different turbine would be running) for small changes in the wind speed. It is considered more important to have stable optimal set point distributions for small changes in the wind speeds, than having small gains in the power production by allowing downwind turbines to start before their upwind turbines. This is the reason for keeping the second penalty function in the objective function.

### 4.2.2 Optimised set point distribution for row wind farms with two turbines

A suitable objective function has been defined and `fminunc()` is used to find the optimal set point distribution. The first wind farm where the optimisation

algorithm is applied is the row wind farm with two turbines. Only the set point of Turbine 1 is optimised as Turbine 2 should be run in nominal operation.

The problem is solved for wind speeds form 3 m/s to 15 m/s with steps of 0.1 m/s, meaning 121 problems are solved for the small row wind farm. When solving the problem the optimiser needs an initial guess. The initial guess should obviously be as close to the true optimum as possible. The problems are solved in the order of their wind speeds. This makes it possible to use the last found solution as the new initial guess. This approach should give good initial guesses as long as the steps in the wind speeds are sufficiently small.

The wind speed decides the order in which the problems are solved, meaning that the problems can be solved in ascending or descending order. It shouldn't matter in which order the problems are solved, if the problems are convex and have a sufficient curvature all over the solution space. To test if this indeed is the case the problems are solved twice. The first time the problems are solved it will be in ascending order, meaning the initial guess will be slightly too low compared to the true solution. This method will be known as the "forward scan" (FS). Afterwards the problems are solved in descending order meaning the initial guess are too high. As the problems are in reversed order this method is known as the "reversed scan" (RS).

In Figure 4.1 the results from solving the 121 problems from different wind speeds using the forward scan method are shown. At the left plot the solutions for all the wind speeds are shown. As a reference the set points from the MPPT strategy is also shown. It can be seen on the blue and black dotted line that the average load on the turbines are higher using the optimised set point from 3.8 m/s to around 11 m/s compared to the MPPT strategy. Above 11 m/s it is optimal for both strategies to have Turbine 1 running on full load, meaning that the strategies are the same for wind speeds above this level .

Below 3.8 m/s both strategies are also the same as both of them let the Turbine 1 extract as much energy from the wind as possible. After 3.8 m/s the Turbine 1 is down regulated when using the optimised set points. As Turbine 1 is down regulated the wake deficit doesn't reduce the wind speed in front of Turbine 2 below the cut-in speed allowing the turbine to start producing power. Since the average load is higher for the optimised set points the loss in power from down regulating Turbine 1 is less than the gain in power from starting Turbine 2.

Looking at the average load for the optimised set points, at the right plot on Figure 4.1, it appears that a gain in average power could come from down regulating Turbine 1 for wind speeds lower than 3.8 m/s. These issues will be investigated further after the results from the reversed scan has been analysed.

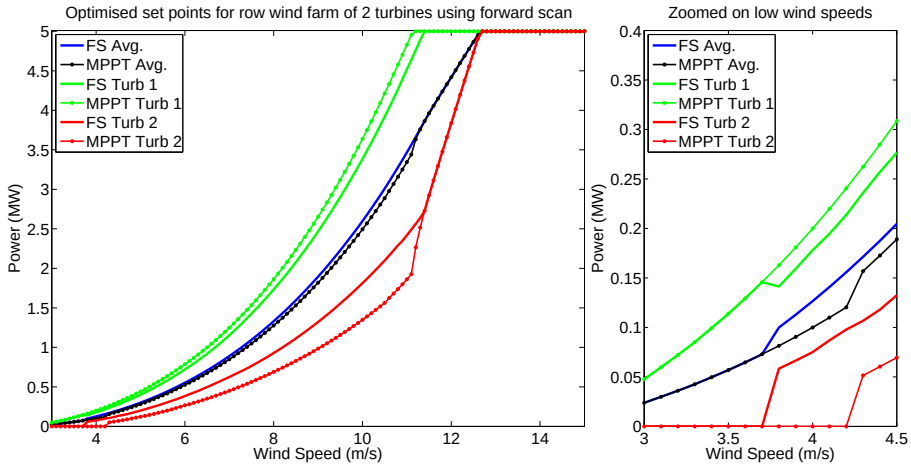


**Figure 4.1:** Optimised set points using the forward scan method compared with MPPT. Left side is the solution for 3 to 15 m/s. Right side is zoomed on the solution from 3 to 4.5 m/s.

At Figure 4.2 the optimised set points for the same 121 problems are shown and the problems are solved using the reversed scan method. Comparing the solutions from the forward and reversed scan only small differences are noticed. Looking at the plot for lower wind speeds it is seen that Turbine 2 is switching between running and not running for wind speeds around 3.5 m/s to 4 m/s. It is seen on the blue curve that for 3.6 m/s the total power production is higher when down regulating Turbine 1 and having two turbines running. Looking at the solution for 3.7 and 3.9 m/s the optimiser found it optimal to have only one turbine running, which obviously is wrong as the curve for the average production clearly indicates it is beneficial to have two turbines running in this case.

An issue with optimising the problems was found when analysing the forward and reversed scan solutions. Local optimums seems to appear for wind speeds around 3.5 to 4 m/s. Since only one set point is optimised for this wind farm it is easy to show the solution space for a given wind speed. This will shed light on when its optimal to have two turbines running and why the optimiser doesn't find the same solutions using forward and reversed scan.

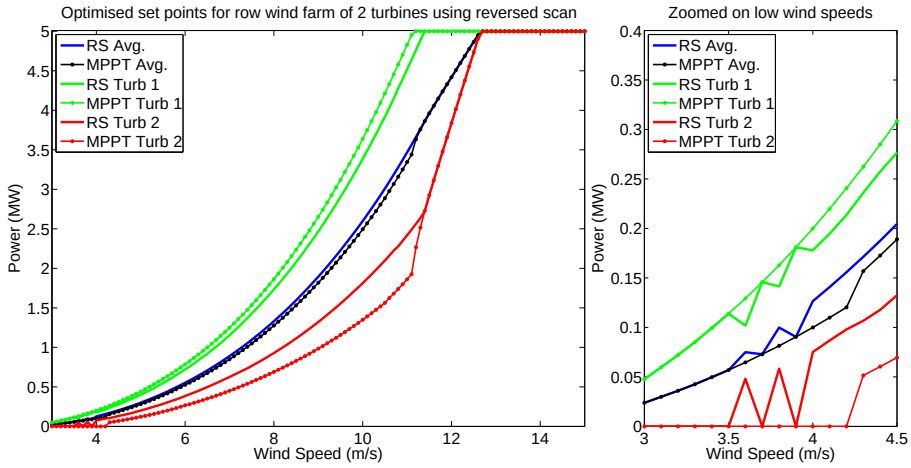


**Figure 4.2:** Optimised set points using the reversed scan method compared to MPPT. Left side is the solution for 3 to 15 m/s. Right side is zoomed on the solution from 3 to 4.5 m/s.

### 4.2.3 Solution space for a row wind farm with two turbines

Only one set point needs to be optimised for each wind speed. Since the problem is very small a method to analyse the solution space for a given wind speed is to evaluate the objective function for a number of set points. This will give a good idea of how the solution space looks and show the curvature and optimums of the objective function. This is only possible as long as the problem consists of optimising at most two set points.

On Figure 4.3 the solution space for the problem is shown for wind speed 3.4 and 3.8 m/s. Each plot shows the power production on each turbine as a function of the set point given to Turbine 1. It is seen that when the set points given to Turbine 1 increases less wind is available for Turbine 2 and the production decreases. The blue curve shows the cumulated power where non of the penalty functions are added and the magenta curve shows the objective function, i.e. the cumulated power where penalties are added.

On the right plot on Figure 4.3 it clearly shows that the objective function and the cumulated power are the same when Turbine 1 produces more power than Turbine 2 and it is possible for Turbine 1 to produce the demanded set point. Whenever one of these requirements aren't met the objective function is penalized. Whenever too high set points are given the cumulated power is constant whereas the objective has curvature, meaning the penalty function

fulfills its purpose. It can also be seen that the penalty added for given too high set points starts with being quadratic and at some point becomes linear.

When the wind speed changes from 3.4 to 3.8 m/s it is no longer optimal to have only one turbine running, meaning that at 3.8 m/s it is optimal to down regulate Turbine 1, so that the wind speed in front of Turbine 2 is above the cut-in wind speed. Looking at the left plot it can be seen that the objective function almost has the same value when Turbine 1 is down regulated to its optimum and when it is running on full load, meaning that close to 3.4 m/s curtailing upwind turbines starts to be a better strategy than MPPT.

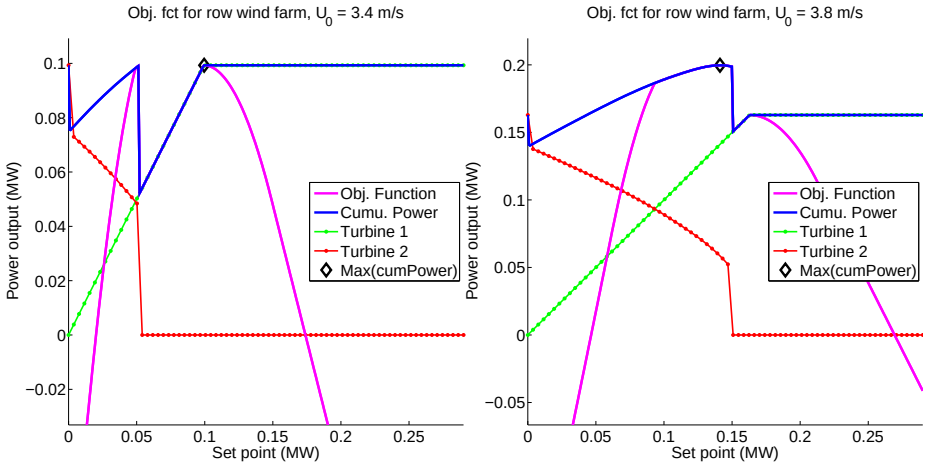


**Figure 4.3:** Plot of solution space of optimisation problem for the row wind farm with two turbines. The objective function and cumulated power are plotted as a function of the set point given to Turbine 1. On the left plot the wind speed is 3.4 m/s and on the right side the wind speed is 3.8 m/s.

On Figure 4.1 and 4.2 it was shown that the optimiser had difficulties in finding the true optimum of the objective function for low wind speeds. At Figure 4.3 it is clear that both the objective functions and the cumulated powers have local optimums. These local optimums are most likely the reason why the reversed scan switched back and forth from having two turbines running for low wind speeds and why the forward scan didn't find it optimal to have both turbines running before 3.8 m/s. It is unfortunate that the objective function has local optimums for some wind speeds as it complicates finding the true optimum. An analysis is carried out to find out if the local optimums can be removed or a method can be developed to ensure that the optimiser always finds the global optimum of the objective function.

## 4.3 Analysis of local optimums in the objective function

In this section two things will be investigated, namely the origin of the local optimums and a method to avoid them. Two things are suspected to affect the local optimums. The first is that the turbines can't produce energy when the wind speed is below 3 m/s. This is the reason that the local optimums appear on the objective function. This can be seen on both the plots on Figure 4.3. Looking at the two optimums on the right plot it can be seen that for set points slightly higher than the true optimum global a discontinuous drop in objective function is observed. The drop comes because Turbine 1 doesn't let enough wind pass to Turbine 2 for it to be running. This gives an extra optimum in the cumulated power, because when the set points are increased hereafter the cumulated power starts to increase again, as letting less wind pass to Turbine 2 has no consequences anymore. The extra local optimums disappear when the wind speed increases, so that the wind speed in front of Turbine 2 can't be reduced to less than the cut-in wind speed even with Turbine 1 running in nominal operation.

The second thing which affects the local optimum is that turbines don't start producing 0 MW at the cut-in wind speed but start at some small value. This causes the objective function to become discontinuous when the wind speed in front of Turbine 2 is less than the cut-in wind speed. The bigger power production is at the cut-in wind speed the bigger the discontinuity is.

Finding the true optimal solution to the problems might be easy for the small row wind farms but as more turbines are added more local optimums will occur and finding a simple method to find the global optimum becomes complicated very quickly. Even though local optimums disappear when the wind speed increases the issue will still occur for higher wind speeds as the size of wind farms increases and higher wake deficits are observed.

As the problems with local optimums are caused by the power curve from the turbine model it is difficult to find methods that will always find the true optimum without changing the turbine models. Penalty functions are difficult to apply in this case. Making the proper changes to the turbine model might solve the issues but would give an unrealistic model. However, the gain from having a turbine model not giving local optimum in the objective function is robust solutions for all initial guesses. Having a robust solution for changing wind speeds is important if this strategy ever is to be implemented for test purposes.

Two different test turbine models have been implemented to see if the local opti-

mums can be removed. In the first test model a new cut-in region is introduced for wind speeds between 0 and 3 m/s. When the wind speed is 0 m/s the power production should be 0 MW and at the cut-in speed the production should be the same as the production at cut-in speed for the real model. In the cut-in region it is assumed that the available power depends cubic on the wind speed like the kinetic energy in the wind. Hence, the available power in the cut-in region is found by fitting a third order polynomial (with a third term only).

In the second test model the low region is removed and the mid region is extended all the way 0 m/s. This approach will violate the constrain from the cut-in rotor speed and give an unrealistic turbine model whenever the wind speed is below around 6 m/s. To test if any of the modifications of the turbine model has removed the issue with local optimums the solution space is plotted for 3.8 m/s for both test models.

On Figure 4.4 the solution space for the two test models for 3.8 m/s is shown. On the left plot it can be seen that adding the cut-in region doesn't solve the problem as two optimums are still seen on the objective function. The local optimums occur because the slope of the power curve changes when Turbine 2 changes from being operated in the cut-in region and the low region. The two optimums are close to each other and no discontinuities are seen on the objective function. For the test model with an extended mid region the objective function has only one optimum. The reason that no optimums occurs is that no transitions in operating regions are present, giving a smooth objective function.

The results from modifying the turbine model shows that to get rid of the local optimums it is not sufficient to have a model which can produce power at any wind speed higher than 0 m/s and will start producing from 0 MW but the slope of the function will also need to meet some requirements. The model with extended mid region actually solves the problem with local optimums but this model is unfortunately considered quite unrealistic as deviations from realty are seen from 6 m/s and below. No good solution has been found to the problems with local optimums.

## 4.4 Set point distributions for larger row wind farms

The optimisation problem for finding the optimal set point distribution for a small wind farm was shown not to give robust solutions when the initial guesses changed, due to local optimums. The number of local optimums is expected to increase as the number of set points increases, meaning that the solution

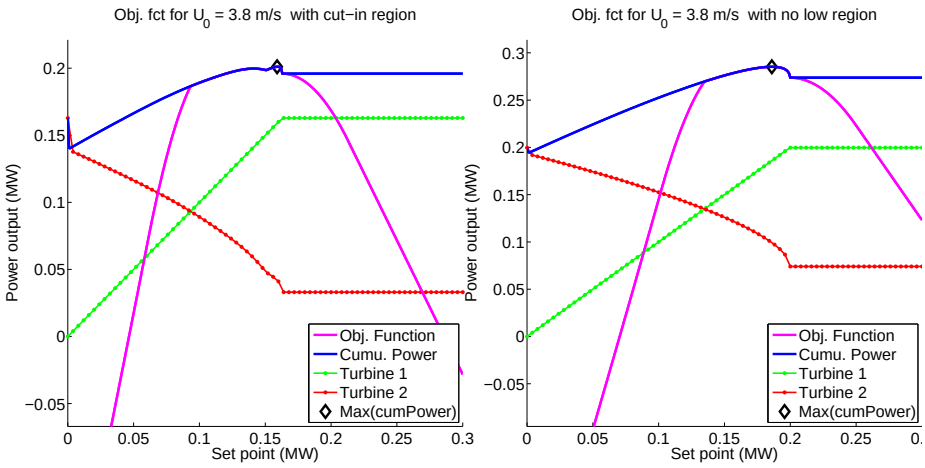


**Figure 4.4:** Solution space of optimisation problem for row wind farm with two turbines with modified turbine model for 3.8 m/s wind speed. Left plot: the cut-in region has been added to turbine model. Right plot: The low region has been removed and the mid region extended to 0 m/s.

to the problem should be even more dependent on the initial guess given to the optimiser. To address what happens for larger wind farms the optimisation problem has been solved using the forward scan method for a row wind farm with five turbines standing with five rotor diameters distance to each other. The results for finding the optimal set point distribution for wind speeds from 3 to 15 m/s can be seen on Figure 4.5.

The results from optimising the set points for the row wind farm doesn't look very convincing. Some of the turbines are being started and shut down repeatedly for low wind speed, as it can be seen in the right plot on Figure 4.5. This is also a problem for the MPPT strategy. The problem occurs when Turbine 1 is started and the wind speed is reduced for all downwind turbines to below the cut-in speed. When the wind speed increases the first downwind turbine, which has more than the cut-in wind speed in front of it, is the last turbine as the distance to Turbine 1 is largest. This issue could be solved by not starting a turbine if any upwind turbines are not running. This would, however, change the optimal set point distribution some for low wind speeds. Also in reality turbines are not allowed to be down regulated when producing less than some percentage of the rated power. As the issue with turbine is only present for set points around 4% of the rated power, down regulating at these wind speeds might not be allowed anyway.

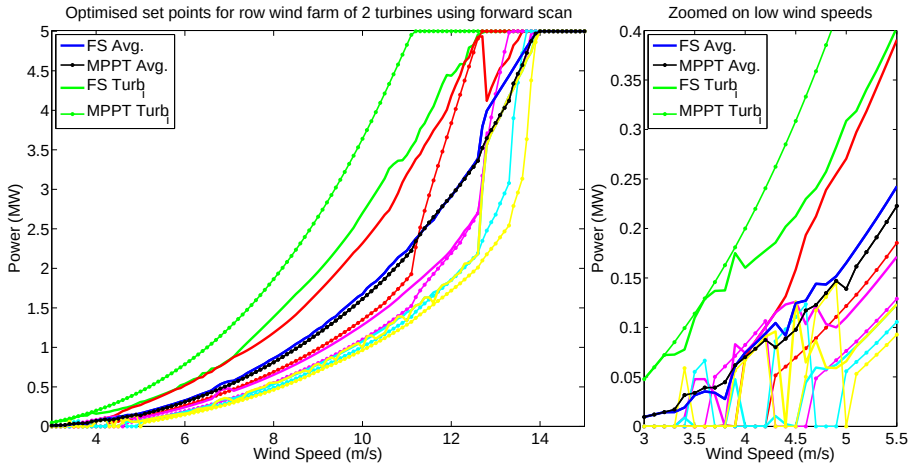


**Figure 4.5:** Optimised set points using the forward scan method compared with MPPT. Left side is the solution for 3 to 15 m/s. Right side is zoomed on the solution from 3 to 5.5 m/s. The solid lines are the optimised set points and the dotted lines are set points using the MPPT strategy. (T1 = green, T2 = red, T3 = cyan, T4 = magenta, T5 = yellow)

On the left plot on Figure 4.5 it is shown that for wind speed less than around 12.5 m/s the forward scan is not beating the MPPT strategy by much. Above this speed the second turbine is suddenly down regulated causing a significant increase in cumulated power. As the solution space should be quite smooth this is not as expected. It indicates the set points below this wind speed hasn't been optimised to its global optimum. It is not possible to show the solution space very well for this problem as four turbines are optimised. It was shown that the reversed and forward scan didn't find the same solutions for the row wind farm of two turbines. The reversed scan is therefore used on the problem to see if it performs better.

On Figure 4.6 the solution for the reversed scan is shown on the left plot. The start issues for low winds are still present as expected. The performance of the reversed scan is seen to be significantly better than the MPPT strategy. For wind speed between 4 and 11 m/s Turbine 1 is down regulated around 20% compared to the MPPT strategy. Turbine 2, 3, 4, and 5 are kept at the same set point until Turbine 1 is running on full load, hereafter Turbine 2 is kept a bit higher than the last three turbines. Curtailing the front turbines allow an increase in the average production for 6 m/s on 29% and 19% at 11 m/s compared to MPPT. The fact that the last four turbines are given the

same optimal set point indicates that the wind speed in front of each turbine might have reached a equilibrium. This is somewhat in line with the results from Figure 3.3, where the normalised wind speed in front of turbines on a row reached it equilibrium around turbine 3-4.

Turbine 1 is being down regulated from full load and then slowly set back to full load at around 12 m/s (start at 11.9 and ends after 12.2). The average power isn't affected noticeably but it seems unlikely that the true optimum has been found. Looking at the exit flag from the optimiser shows that it converged for all these wind speeds. The algorithm didn't converge for 11.8, however which seems counter intuitive as the solution for the wind speed is running Turbine 1 on full load.

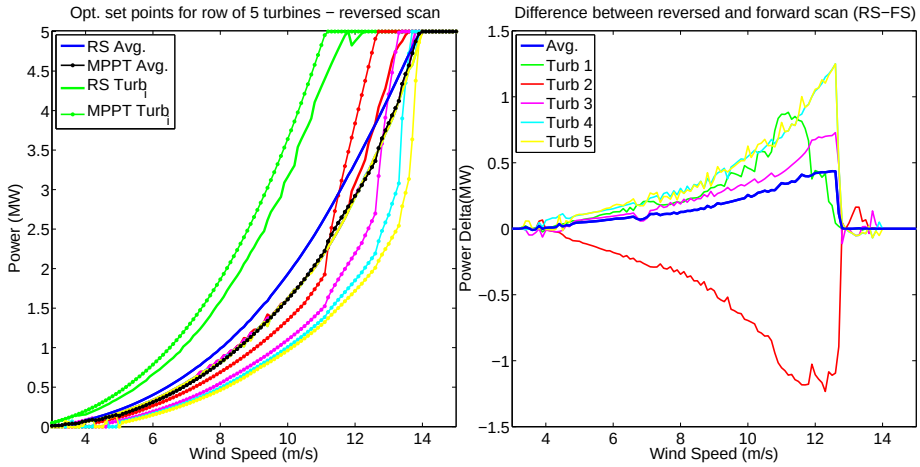


**Figure 4.6:** Left plot: Optimised set points using the reversed scan method for 3 to 15 m/s. Right plot: Differences in the solutions using the reversed and forward scan.

Looking at the right plot on Figure 4.6 the difference between using forward and reversed scan is plotted for 3 to 15 m/s. It is seen that the reversed scan is giving a better solution than the forward scan until the forward scan suddenly down regulates Turbine 2. Turbine 1, 3, 4, and 5 are in generel operated at a higher set using reversed scan which results in a higher average production.

The differences seen between the forward and reversed indicates that the optimiser has issue converging to the right optimum. The solution using forward scan were consistent (but a wrong optimum was found) until 12.5 m/s indicating that a local optimum could exist. The issue with the reversed scan down regulating Turbine 1 around 12 m/s is suspected to come because of lack of cur-

vature on the objective function. Turbine 1 is down regulated significantly but the change doesn't seem to affect the average power. This could be because the solutions in this region has only little curvature making it difficult for the optimiser to find the true optimal distribution. As the average power isn't affected significantly this is mainly an issue if this strategy were to be implemented in a control system. Evaluating the annual gain for curtailing upwind turbine versus MPPT wont be affected by this issue.

## 4.5 Perturbation of initial guesses

If curtailment of upwind turbine was to be tested the solutions should be robust. The forward scan showed really poor performance and the reversed scan had inconsistencies. To give even more robust solutions an extra step is made when solving the problems. Serveral initial guesses are made instead of just using the previous solution as an initial guess. This will allow the optimiser to come from different places and hopefully one of the initial guess will converged to the true optimum. Five initial guesses are defined where the first is the previous solution. The next initial guesses are made as random perturbation of the previous solution. The perturbations are defined as:

$$\mathbf{x}_i^* = \mathbf{x}_{prev} + \mathbb{U}(-0.25, 0.25)\max(\mathbf{x}_{prev}) \tag{4.8}$$

where $\mathbf{x}_i^*$ is the $i$'th initial guesses, $\mathbf{x}_{prev}$ is the optimal set points for previous iteration and $\mathbb{U}(-0.25, 0.25)$ is the uniform distribution from -0.25 to 0.25. This way to perturbing has been decided due to good performance, when it was tested against other methods. Uniform distributions with smaller and large ranges have been tested as well and the chosen distribution performed the best. Testing multiple perturbations showed that having more than five perturbations didn't improve the results in most cases.

Using five initial guess gives five solutions to each problem where the one with the highest cumulated power is chosen in each iteration. Having to solve the each problem five times in each iteration obviously increases the run time. The results from optimising the row of five turbines while perturbating the initial guesses can be seen on Figure 4.7

The optimised set points for the perturbed initial guesses are very similar to the ones found with the reversed scan method but are more stable. Turbine 1 is not down regulated around 12 m/s as for the reversed scan indicating the method with perturbing the initial guesses makes the solutions more robust. Looking at the left plot on Figure 4.7 shows that only small deviations are seen between the individual turbines for the two methods. The deviations for the turbines

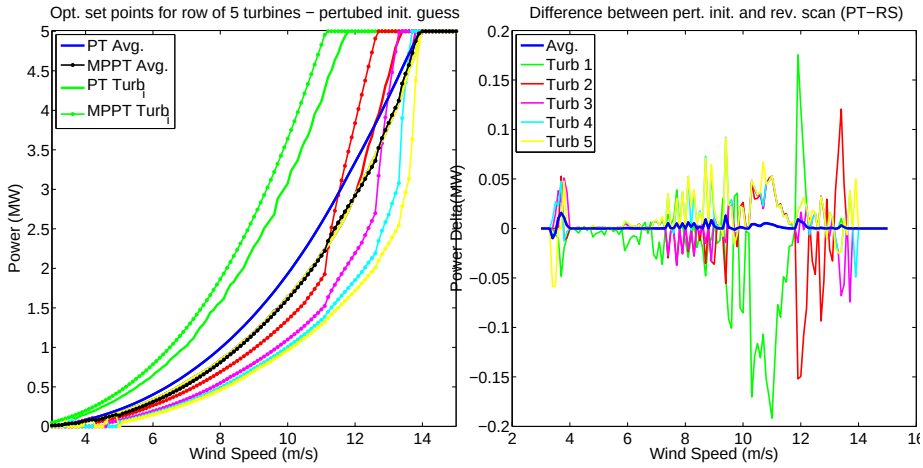


**Figure 4.7:** Left plot: Optimised set points using the perturbed initial guesses for 3 to 15 m/s. Right plot: Differences in the solutions using perturbed initial guesses and reversed scan.

doesn't seem to affect the cumulated power as almost no differences (in the order of $5 \cdot 10^{-2}$) is seen in the cumulated power. This indicates the cumulated power is not sensitive to small changes in the turbine set points, meaning that solution space could lack curvature for higher wind speeds.

## 4.6 Bundling of set points

The increased number of set points to be optimised has shown some new issues with robustness of the solution. Perturbing the initial guesses showed little improvement but came with a price of significantly increased run time. Going from one to four set points to optimise made it harder for the optimiser to find the true optimums. For larger problems this issue is expected to become even more problematic and using only five perturbations might be insufficient. Hence, it would be advantageous to be able to reduce the number of set points to optimise to give faster and more stable solutions.

It was noticed that the optimised set points for the last three turbines was almost the same set point for most wind speeds when applying both the reversed scan and perturbed initial guesses. In both cases these set points were optimised individually but it seemed optimal to have them running at the same load. Instead of optimising all set points individually, it is tested whether more robust

solutions can be obtained if some turbines are given the same set point instead of operating them at different levels.

A test is made were only a number of the most upwind turbines are optimised individually. The rest of the turbines in the row are given the same set point, meaning only one set point is optimised for all of them. "Bundling" the last turbines together (giving the same set point) will reduce the number of set points to be optimised while hopefully not affecting the cumulated power outputs.

Several tests on how to bundle the turbines have been made, including testing whether the last turbine in a row should be running nominal or have its set point bundled with the rest of the downwind turbines. These tests indicated that bundling the last turbine with the other downwind turbines gave best best performance, both when testing a row of five and eight turbines. Test of how many of the downwind turbines should be bundled has also been made. The results from bundling Turbine 4 and 5 can be seen on the left plot on Figure 4.8, while the results from bundling Turbine 2 to 5 can be seen on the right plot (meaning only two set points are optimised).

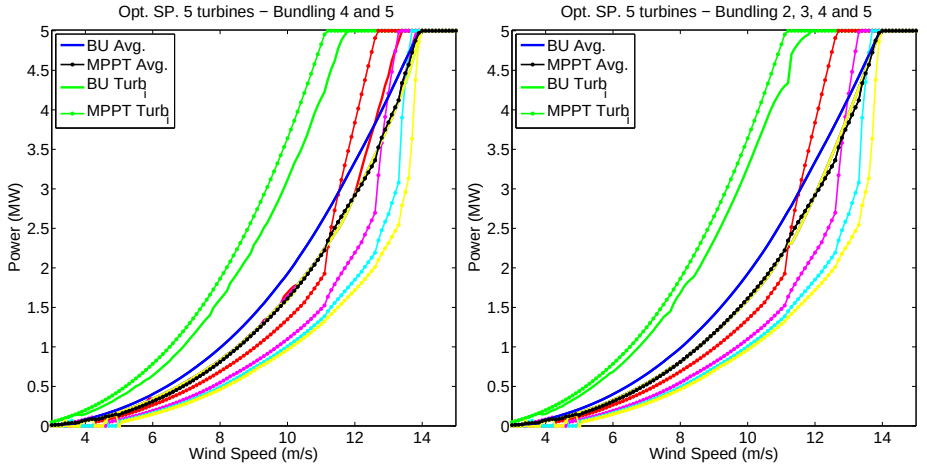


**Figure 4.8:** Left plot: Optimised set points when bundling Turbine 4 and 5. Right plot: Optimised set points when bundling Turbine 2, 3, 4 and 5.(T1 = green, T2 = red, T3 = cyan, T4 = magenta, T5 = yellow)

The results from bundling the last two turbines shows a smoother solution. The last three turbines in the row are operated almost identically even though Turbine 3 is being optimised individually. However, bundling this turbine as

well gave a less smooth solution. The cumulated power for these solution are on average 0.03% better than the reversed scan, but have a more robust solution space. Looking at the right plot on Figure 4.8 it clearly shows that only two lines from the optimised set points are visible as Turbine 2, 3, 4 and 5 are kept running at the same level. This gives a quite smooth solution even though Turbine 1 behaves a little suspicious, where a jump in the set point is seen going from 11.3 to 11.4 m/s. This solution is on average 0.11 % lower than the reversed scan, the run time is however less than a third and due to the bundling the solution is considered more robust because the solutions are very smooth.

Tests were also made tests on a row of eight turbines to make sure that adding more turbines to the row didn't affect how many of the front turbines should be optimised individually for good performance (plots are omitted). The results showed that only optimising the first three turbines individually gave more unstable and (slightly) worse results than optimising only the first two turbine individually. Optimising only the first turbine individually lowered the run time of a factor three compared to optimising three turbine invidually. This resulted in a loss of only 0.24%. Comparing the cumulated power for the reversed scan and bundling method for the row of eighth turbines shows that bundling the turbines gives a decrease of 0.43% in cumulated power. This is a quite insignificant loss, considering only one forth of the set points was optimsed. The solutions when optimising only the first turbine individually where also very smooth and without jumps. This indicates that for larger wind farms it might be beneficial for robustness and CPU time to only optimise the first turbine individually. This can be done with only insignificant loss in the cumulated power.

Bundling the most downwind turbines has showed to be beneficial if a fast and robust solution is wanted. A risk of getting a slightly worse cumulated power is introduced, though. If set points were to be optimised for large wind farms with e.g. 80+ turbines it might be very beneficial to use bundling of turbines as the the overall power productions wouldn't change significantly, but much faster and robust solutions would be obtained.

Chapter 5

# Wind farms in two dimensions

In the previous chapter row wind farms was optimised and the results were analysed in details. The analysis was used to define different methods to improve the performance of the optimiser. The methods will be used in this chapter to analyse wind farms in two dimensions. Wind farms will be analysed both for different wind speed and directions.

## 5.1 2x5 wind farm

The first wind farm to be analysed in this chapter is consisting of two rows of five turbine each. The distance between turbines are five diameter in each direction. The direction of the wind will be fixed at 270 degrees (where 0 degrees is north and 270 degrees is west) for this entire section. The layout of the wind farm can be seen on Figure 5.1. The wake effects are largest possible for this layout given the wind direction, as the turbines in each row stand in full wake of each other. The wakes from the front turbines are seen not to expand enough to cause wake deficits for turbines in the other row. This problem is very similar to the ones solved in Chapter 4. The optimal set point distribution for each row in this problem should be the same as for a single row of five turbines, as no cross-wind

wake interaction is happening.

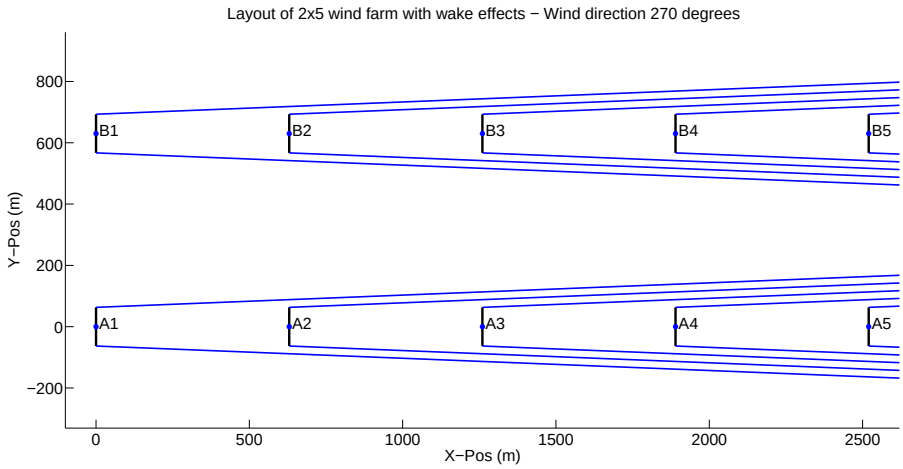


**Figure 5.1:** Illustration of the layout of the 2x5 wind farm with wake effects. The rotors are marked with blue dots and the blades with black lines. The blue lines starting at the ends of each blade defines the area behind the turbine that is affected by the turbines wake. Rows are named with letters and column with numbers.

The optimal set point distribution will be found for wind speeds from 3 to 15 m/s as done previously. The last turbine in each row are the only ones not having any downwind turbine, meaning eight set points must be optimised for each wind speed. The increased number of set points to optimise increases the run time by more than a factor 5. The reversed scan method will be used without perturbation or bundling to solve the optimisation problems for this entire chapter. The reason for not using bundling of turbines is that no algorithm has been developed to detect what turbines stand in the wake of each other. Developing an algorithm to detect patterns of the wake effects from all the turbines in wind farm with changing wind direction is difficult, as the layouts of wind farms not always are rectangular or defined by some nice pattern. The reduced run time and good robustness of the bundling method would otherwise have been suitable for this problem.

The optimised set point distributions for each row in the wind farm has been plotted on Figure 5.2. The two distributions look completely similar to each other as expected. This indicates that the optimiser isn't too affected by the difficulties seen in Chapter 4. The optimiser did have some issues converging for some winds, so the number of maximum function evaluations had to be

increased significantly compared to the setting used for the 1x5 row wind farm.

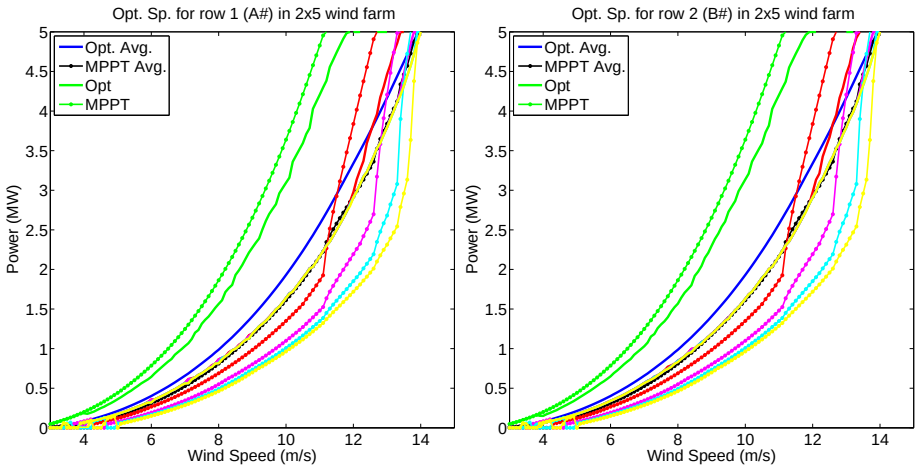


**Figure 5.2:** Optimised set points for 2x5 wind farm with wind speed from 3 to 15 m/s, using the reversed scan method. Left plot: Set points for row A. Right plot: Set points for row B. (T1 = green, T2 = red, T3 = magenta, T4 = cyan, T5 = yellow)

The optimised set point distribution for each row is also very similar to the reversed scan solutions for the 1x5 wind farm. The differences in the optimal set point for each turbine in row A and B have been plotted on the top left plot on Figure 5.3. No differences is seen to be large than 0.05, which most likely is caused by numerical issues. On the top right plot the differences in the set point from row A and the reversed scan solution for the 1x5 row wind farm is seen. The largest difference is a little less than 0.2 and is caused by the drop on Turbine 1's set point for 11.8 m/s for the 1x5 wind farm that was seen on Figure 4.6. Otherwise all difference are suspected to be due to numerical issues.

The relative gain of curtailing upwind turbines compared to MPPT is shown on the bottom plot on Figure 5.3. At around 3.5 m/s MPPT is actually better than curtailing which is caused by the issues with local optimums while not all turbines are running. The relative gain is largest for 5 m/s where the gain is around 50%. 50% gain is a very good performance but it should be kept in mind that this result is based on the wind direction giving the largest wake effect from this farm. However, the actual gain for these wind speeds are modest as the cumulated power for 5 m/s is around 1 MW. The relative gain decreases asymptotic as the wind speed increases, until Turbine 1 start to run on full load.

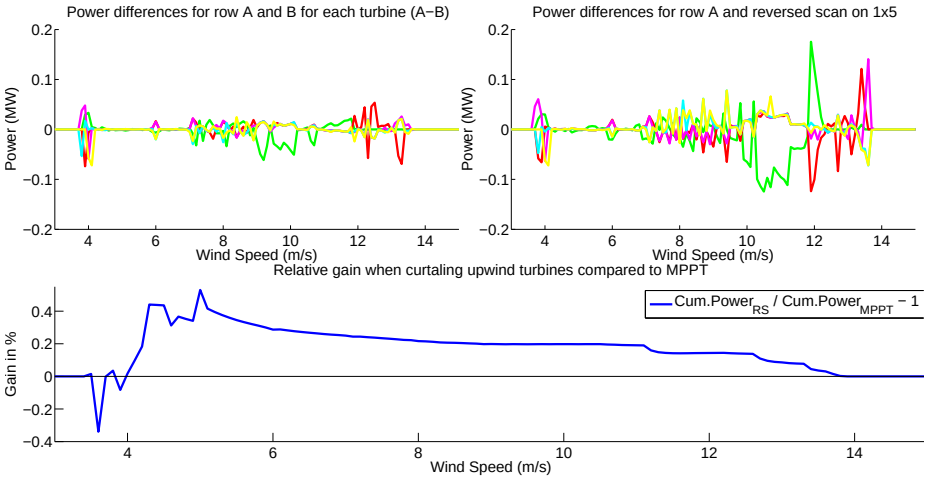


**Figure 5.3:** Top Differences in optimised set points for each turbine. Top left plot: differences between row A and B from the 2x5 wind farm. Top right plot: Differences between row A and reversed scan for the 1x5 wind farm. (T1 = green, T2 = red, T3 = magenta, T4 = cyan, T5 = yellow). Bottom plot: Percentage gain using the optimised set points vs. MPPT.

At this point the relative gain is around 20% but drops fast to 14% and starts to decrease asymptotic again. This happens every time the wind has increased enough for having a new turbine running on full load.

## 5.2 5x5 wind farm for different wind directions

The impact of changing wind direction on a large square wind farm will be analysed in this section. A 5x5 wind farm with five diameters turbine spacing in each direction is chosen for this analysed. Instead of solving the optimisation problems for many different wind speeds and one wind direction the wind speed will be fixed and direction changed in this section. The farm is analysed for 10 m/s wind speed and with wind speeds changing from 270 degrees to 360 degrees with 3 degrees steps. The optimal set point distribution of a square wind farm (with equidistant turbine spacing and same number of turbines in each direction) will repeat it self every 90 degrees due to the layout of the farm. Furthermore, the solutions from direction 0 to 45 will be same as for 45 to 90, just in reversed order. So finding the optimal set point distribution for wind directions between 270 and 315 degrees is enough to calculate to solution for all directions.

The optimal set point distributions for different wind directions can be seen on Figure 5.4. The set points of all 25 turbines has been plotted to illustrate that the turbines have a tendency to cluster near some set points. E.g. for 297 degrees where turbines are operated either at nominal operation, just below nominal operation or at around 2.5 MW. This is as expected as patterns in the wake effects should occur. The solutions are seen to be symmetric around 315 degrees as expected (the set points has been shifted between turbines, but the average production are almost the same). This indicates that the solver gives the correct distributions for the problems, even though a little difference is seen between 270 and 360 degrees.

The bottom plot show how many turbines is in wake for a given direction. When only few turbines are in wake optimising the set points gives only a small gain. For 270 and 282 degrees only a very little gain is seen compared to MPPT, even though 20 turbine are in wake. This is because a lot of partial wake is seen for those direction, meaning only small wake deficits are caused by upwind turbines. It can be seen that it is due to partial wake as the number of turbines in wake drops to eight at 285 degrees. No big jumps in set points are observed for only small changes in the wind direction. It is a nice feature that the solutions seems relative stable for small changes in the direction of the wind.

The layout of the wind farm can be seen on Figure 5.5 for wind direction 297 degrees. The patterns in the optimal set point distribution that was observed on Figure 5.4 are explained by this layout. Looking at the wake effects it is seen that turbines has either none, one, or two turbines in wakes and no partial wake is occurring. The turbines in nominal operation are the ones with no down- or upwind turbines (e.g. A1, A2, E4, ect.). Turbines with no upwind but at least

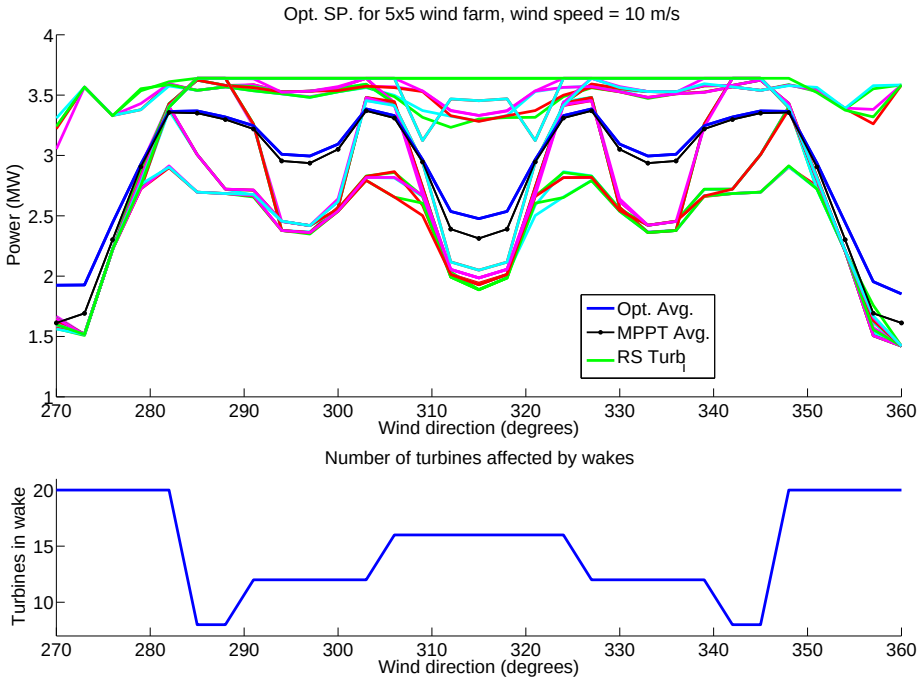


**Figure 5.4:** Optimised set points for 5x5 wind farm at 10 m/s wind speed for wind direction 270 to 360 degrees. Top plot: Optimised set points. Bottom plot: Number of turbines in wake of at least one other turbine

one downwind turbines are down regulated little compared to nominal operation (e.g. B1, B2, E1 ect.). The last cluster of set points are seen for all turbines in wake, no matter if the have only one or two upwind turbines (e.g. B3, C4, E5 ect.). These turbine are operated close to the same set points at 2.5 MW (change very little dependent on number of upwind turbines).

To give a better overview of the optimised set point for the power production on each turbine has been plotted on Figure 5.6 together with the MPPT set points. It clearly shows that the front turbines are down regulated a bit compared to MPPT. The gain from doing so can clearly be seen on all turbines in wake. However, the relative gain for wind direction 297 degrees is 2.0%.

The relative gain as a function of wind direction can be seen on Figure 5.7. The relative gain is seen be symetric around 315 degrees, which was also seen on Figure 5.4. The gain is highest for 270 degrees (and 360, if the right optimum had been found). The gain is at 19% which is in inline the results from previous

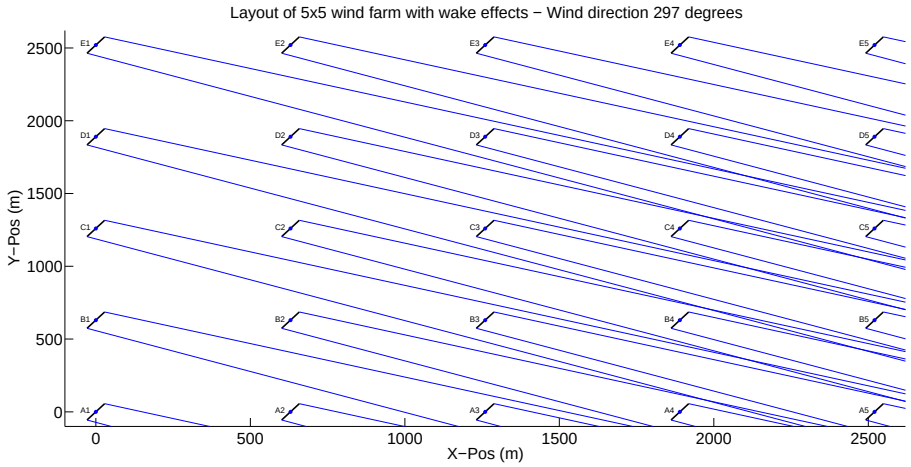


**Figure 5.5:** Layout of the 5x5 wind farm with wake effects for wind direction 297 degrees. The wake effect patterns can be clearly seen on the layout. (NB! axes are not equally scaled)

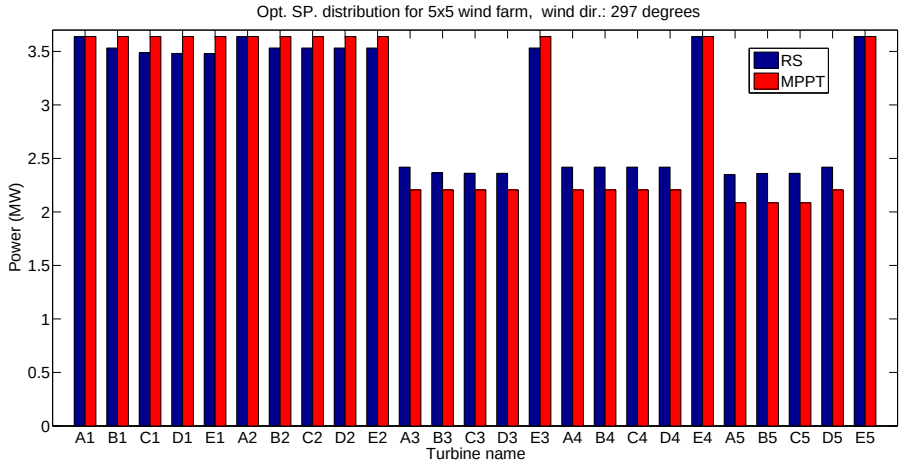


**Figure 5.6:** Comparison of curtailed set points and MPPT for 5x5 wind farm at 10 m/s wind from direction 297 degrees.

section as expected, since the relative gain should be the same the 2x5 and 5x5 wind farm at 270 degrees. As the wind direction changes the relative gain decreases fast as partial wake starts to occur until eight turbines are in wake. When less wake effects are observed the relative gain is expected to decrease as less improvement of the farm control is possible. If all turbines was in free

wind the cumulated power would be 91.0 MW. For 282 degrees the cumulated power is 84.1 MW for the optimised set points and 83.9 MW for MPPT giving a gain of 0.3%. The gap to wake-free production is only at 7 MW. For 270 degrees where the big gain was seen the cumulated power is 48 and 40 MW for curtailing and MPPT, respectively. This gives a gap to wake free conditions on 51 MW, meaning it is possible to improve the performance much more than for 282 degrees, resulting om a much higher gain for the optimised set points.

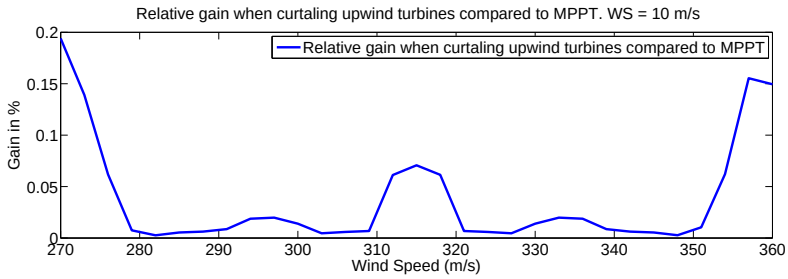


**Figure 5.7:** Bottom plot: Percentage gain using the optimised set points vs. MPPT

Chapter 6

# Sensitivity analysis and structural changes

The purpose of the following chapter is to analyse the effect of changing fundamental elements in the model. The optimal set point distribution will be analysed for a different turbine model and a new wind farm layout. The sensitivity of the wind direction will also be tested in this chapter to give an indication of the losses that might occur if the set points used have been optimised for another direction

## 6.1 CART3 turbine model

The turbine used so-far in this report is the NREL-5 MW reference turbine. To test effect of optimising set points for a different turbine a new turbine model is implemented. The new turbine to be modeled is the NREL-CART3 turbine, the specifications for which are found in [BWF10]. A summary of the relevant specification can be seen in Table 6.1:

| | |
|---|---|
| Rated power | 0.6 MW |
| Rotor diameter | 40 m |
| Hub height | 36.6 m |
| Cut-in, Cut-out wind speed | 4 m/s, 25 m/s |
| Cut-in, Rated rotor speed | 20.0 rpm, 37.1 rpm |

**Table 6.1:** Specifications for NREL CART3 turbine.

This turbine is considerably smaller than the NREL-5 MW turbine. The swept area and rated power are almost a tenth of the 5 MW turbine and the rotational speeds much higher.

The $C_T$ and $C_P$-curves for the CART3 turbines are illustrayed on Figure 6.1. The $C_T$-curves are quite similar to the $C_T$-curves for the 5 MW turbine. The pitch and TSR is plotted for nominal operation from wind speed 4 to 15 m/s. The CART3 turbine is operated for a slightly smaller range of pitch and TSR compared to the other turbine but otherwise the values are quite similar. The $C_p$-curve is seen to have two peaks, but the peak for small pitch values are not affecting the control region. The second peak caused a small modification in algorithm finding the pitch in the low region when maximising $C_P$ for a fixed TSR. Otherwise only the turbine specifications and the $C_P$- and $C_T$-curves have been changed compared to the model used for the 5 MW turbine.

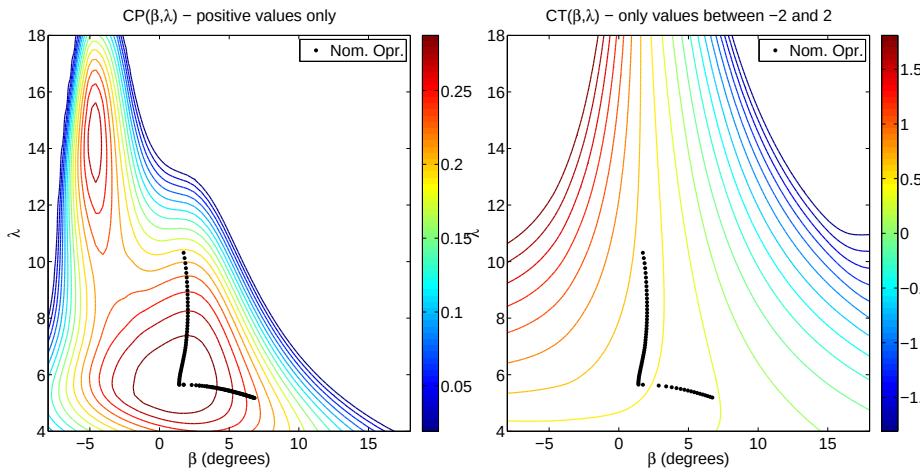


**Figure 6.1:** Comparison of curtailed set points and MPPT for 5x5 wind farm at 10 m/s wind from direction 297 degrees.

At Figure 6.1 the power curve, rotational speed, $C_P$, and $C_T$ values can be seen for wind speed from 4 to 15 m/s when the turbine is operated in nominal operation The rotational speed is seen to be much higher than was observed for the 5 MW turbine. The optimal $C_P$ value 0.31 means that the turbine isn't able extract to more than 31% of the kinetic energy in the wind. The high region for this turbine is gone meaning that the rated rotational speed and rated power is reached for the same wind speed.

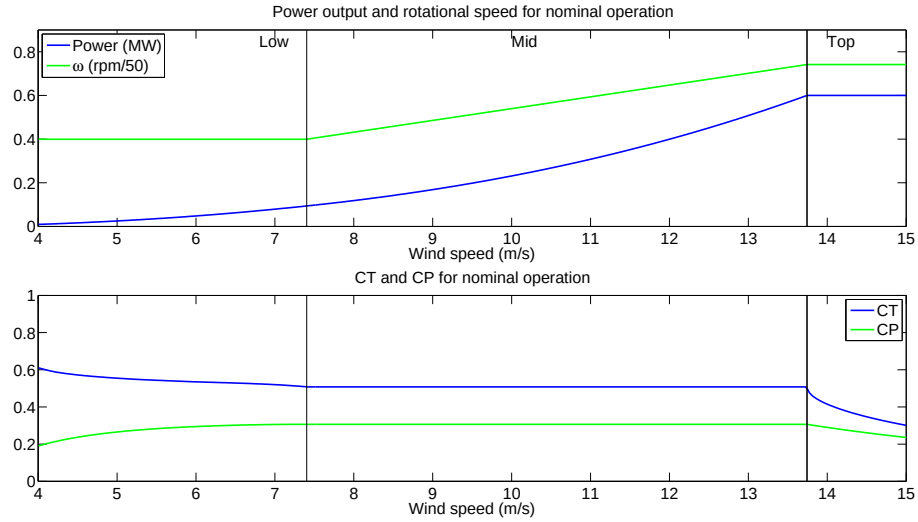


**Figure 6.2:** Top: Power production and rotational speed for the CART3 turbine. Bottom: $C_P$ and $C_T$. Both plots are during nominal operation.

The optimal set point distribution has been found for a row of five CART3 turbines standing on line in the direction of the wind. The turbine spacing is five diameters (of the CART3 turbine). The optimised set point distribution can be seen on Figure 6.3. Curtailing the CART3 turbine gives a higher cumulated power compared to the MPPT strategy but the gain is less than with the 5 MW turbine. It is also noted that all turbines are running full load for wind speeds higher than 16 m/s. Using the 5 MW turbine all turbines were running full load at 13 m/s. The differences could be due to the significantly reduced distance between turbines.

It has been shown that changing the turbine model doesn't cause any new issues for the optimisation problems. This indicates that the proposed method for finding the optimal set point distribution isn't affected by changing the turbine.

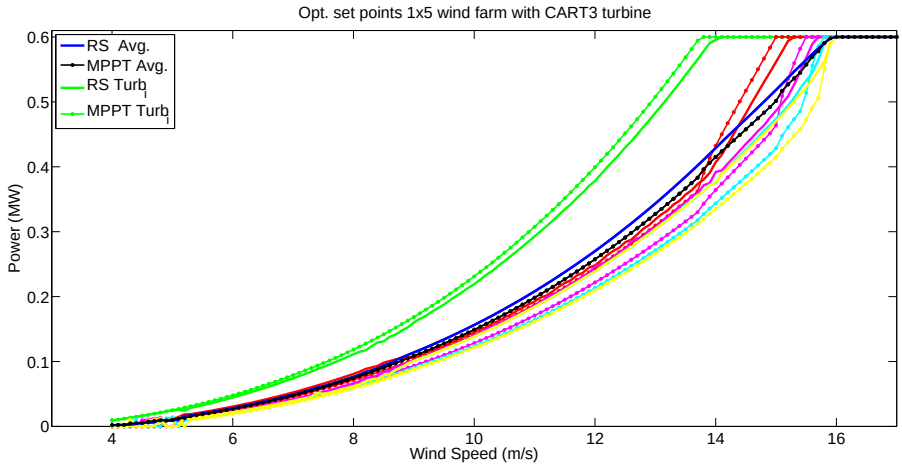


**Figure 6.3:** Comparison of curtailed set points and MPPT for 5x5 wind farm at 10 m/s wind from direction 297 degrees.

However, the gain of optimising set points was shown to be less than for the 5 MW turbine.

## 6.2 Fan-shaped wind farm

The set point distributions has only been analysed for wind farms with quite simple layouts so far. The set points for a fan-shaped 5x5 wind farm will be optimised in this section. The wind farm will be analysed for 10 m/s wind speed and a number of different wind directions.

The more complex farm layout is sure to affect the wake patterns observed and cause the set points to cluster less. The layout of the wind farm for wind direction 315 degrees can be seen on Figure 6.4. It was easy to see a pattern when looking at the wake effects of the squared 5x5 wind farm. This is not the case for the fan shaped wind farm were no patterns occur.

As no patterns were to see in the farm layout the points are expected to more scattered for each wind direction. The optimised set point distribution for 10 m/s can be seen on Figure 6.5. A little tendency of clustering happens around 180 and 360 degrees but otherwise the set points have no tendency of clustering. The number of turbines in wake is also less varying than for the square shaped farm. It is noticed that curtailing the turbines doesn't seem to give much gain

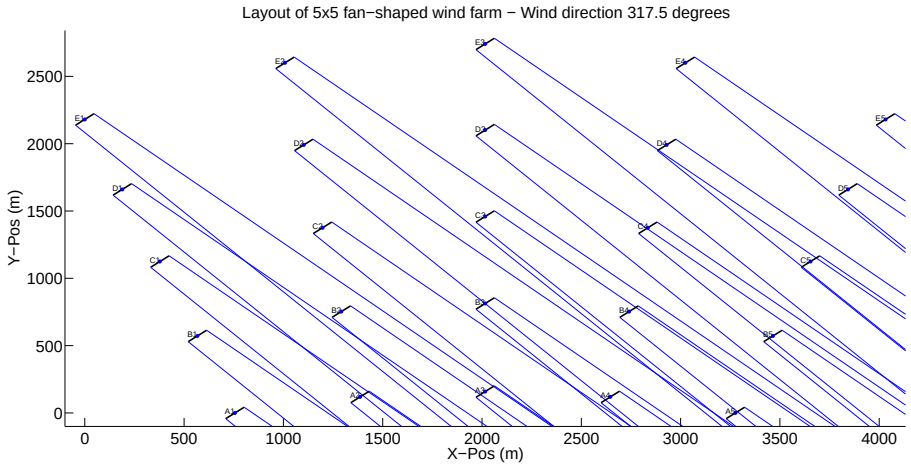


**Figure 6.4:** Layout of the 5x5 fan shaped wind farm for wind direction 297 degrees. (NB! axes are not equally scaled)

compared to the MPPT strategy for this layout. However, the optimised set points are performing better than MPPT for all wind speeds.

It is possible to evaluate the gain of curtailing compared to MPPT for the two layouts, i.e. which layout has the most to gain from curtailing their turbines. It can seen at Figure 6.6 that the gain of curtailing is for most wind direction quite even for the two layouts. However, the gain of curtailing the squared wind farm is much bigger for some directions. This is the case for e.g 180 and 270 degrees, which also are the directions where many turbines stand in full wake of each other.

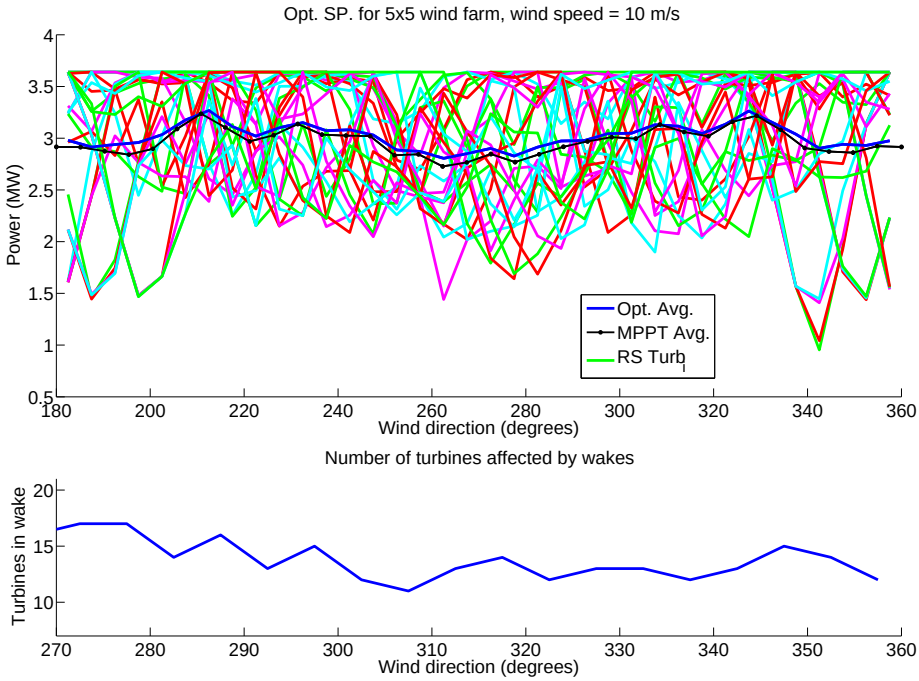


**Figure 6.5:** Optimised set points for 5x5 fan shaped wind farm at 10 m/s wind speed for wind direction 270 to 360 degrees. Top plot: Optimised set points. Bottom plot: Number of turbines in wake of at least one other turbine

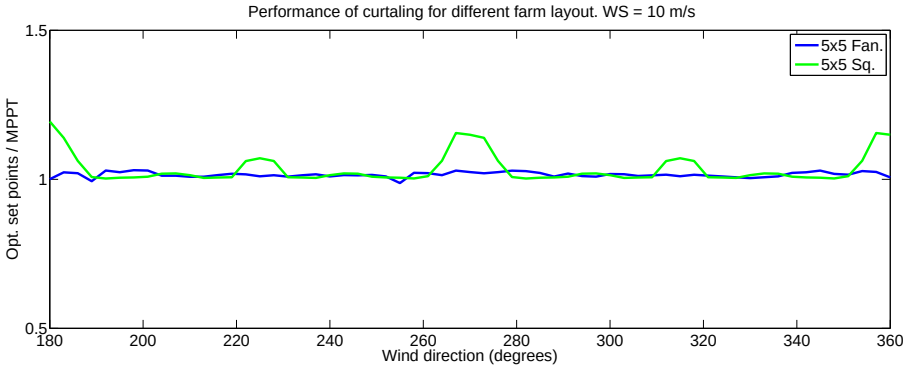


**Figure 6.6:** The optimised set points relative to MPPT for the fan shaped and squared wind farm.

## 6.3 Sensitivity analysis of wind direction

In this section it will be investigated how sensitive the power production is to changes in the wind direction if the set points aren't changed. It will be calculated how much the power production is affected if the set points given to the turbines are optimised for a different direction than the current one.

The set point distributions found in Chapter 5 for the 5x5 wind farm will be extended to cover the wind direction of three and six degrees as well. The power production for the 5x5 wind farm and wind speed 10 m/s is recalculated twice for wind direction 270 to 360 degrees. The set points optimised for direction 273 to 363 is given to turbines in first recalculation of the production. This means the set points are optimsed for a wind direction with an offset of three degrees. In the second recalculation, the set points with an offset of six degrees are given to the turbines.

The results from operating the turbines, with set points optimised for a wind direction with an offset, can be seen on Figure 6.7. The performance of the optimised set points are plotted as a function of the wind direction. The relative gain using the set points with an offset of three degrees optimised for a wind direction with a three offset are seen to be very even with the MPPT (the gain is 0.01%). If the set points with six degrees is used, it gives a loss of 2%.

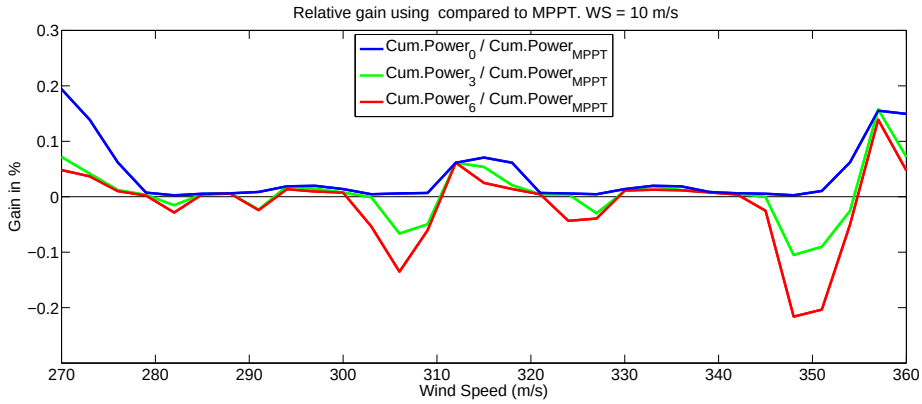


**Figure 6.7:** Relative gain of using power production give

The results from the sensitivity analysis indicates that the optimised set points can be used with a gain compared to MPPT if thy are optimised for a wind direction within three degrees of the current. The results are also of interest if wake meandering is considered (axial movement of the entire wake), or when

considering that wind flows in the real life are much more unstable than what is assumed in the model.

Chapter 7

# Economical effects of curtailing upwind turbines

It has been shown in previous chapters that curtailing upwind turbines can lead to an increased power production for wind farms. It was shown in Chapter 5 that the relative gain from curtailing upwind turbines was very dependent on the wind direction. The economical effect of curtailing turbines will be investigated in this chapter by calculating the annual power production for wind farms given some wind data. Different wind farm layout will be tested and the optimal direction of placing a wind farm will also be found.

## 7.1 Wind Data

The wind data use in this report is forecasted wind speeds with corresponding directions from DMI's HIRLAM model. Predictions for the next 48 hours are given on hourly basis, every six hours. The newest forecasts are always used in this report, meaning no forecast is older than six hours. The data comes from a location off the west coast of Jutland. The data covers the entire year of 2003, consisting of 8760 hours. 72 N/A values were observed in the data (longest period with N/A was 18 hours) and these have been cleansed with linear interpolation.

All the observations are assigned to one of 24 bins, dependent on their wind direction. Each bin ranges 15 degrees and the distribution of the observations for each bin can be seen Figure 7.1. The probability for an observation to belong to bin $k$, $F_k$, has been calculated for 24 of the bins. The most frequent wind direction is west and south-west and the least is north-east.

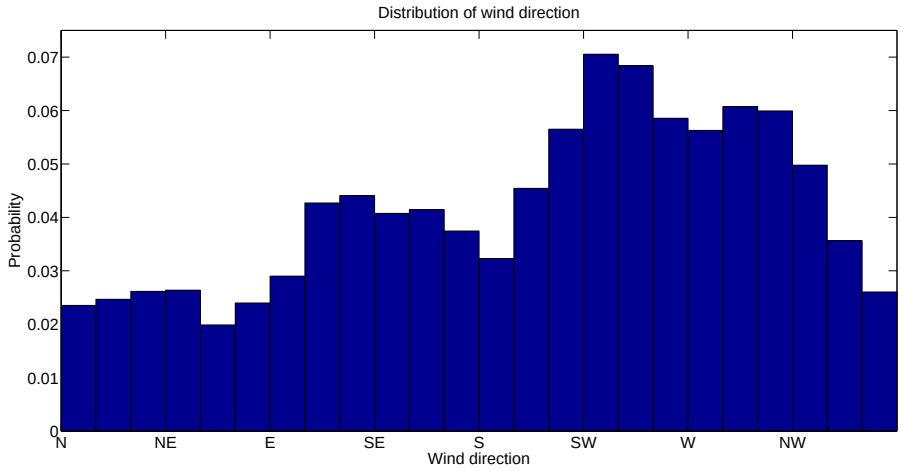


**Figure 7.1:** Distribution of the wind direction for the wind data from 2003.

The wind speed varies from each direction and might have a tendency of being higher for some wind directions compared to others. Since the wind speed cant be assumed to be equally distributed for each direction it is analysed in bins. This means that a wind speed distribution has to be fitted for each bin. The wind speed is assumed to follow the Weibull distribution. A Weibull distribution is fitted for the wind speeds in each bin. The fitted distributions can then be used to calculate the probability for a given wind speed in a given bin.

### 7.1.1 Parameter estimation of Weibull distributions

The two parameters for the Weibull distributions can be fitted to the wind speeds using the probability density function. The Weibull distribution has two parameters $\theta^1$ and $\theta^2$ which is the scale and shape, respectively. The probability functions are defined as:

$$f(\bar{\mathbf{U}}_k;\theta_k^1,\theta_k^2) = \frac{\theta_k^2}{\theta_k^1}\left(\frac{\bar{U}_k}{\theta_k^1}\right)^{\theta_k^2-1} e^{-\left(\frac{\bar{U}_k}{\theta_k^1}\right)^{\theta_k^2}} \tag{7.1}$$

where $\bar{\mathbf{U}}_k$ is the vector of the wind speeds from observations belonging to bin $k$. $f(\bar{\mathbf{U}}_k; \theta_k^1, \theta_k^2)$ is the probability density function fitted to the wind speed in bin $k$. The parameter will be fitted maximising the log-likelihood function. Optimising the parameters to fit the wind speeds for a given bin can be formulated as an optimisation problem:

$$\max_{\theta_k^1, \theta_k^2} \quad \sum_{i=1}^{V_k} \log\left(f(\bar{U}_{k,i}; \theta_k^1, \theta_k^2)\right) \tag{7.2}$$

where $V_k$ is the number of wind speeds in bin $k$ and $\bar{U}_{k,i}$ is the $i$'th wind speed in bin $k$. This problem is solved for each bin and a probability density function is fitted to each bin. The fitted distributions are plotted with their observations for bins close to north, east, south and west on Figure 7.2. The distribution fits the observation quite well, even though the fit for wind speeds from north are a bit skewed. It is interesting to notice that the western winds have very a symmetric flat shape but with considerably high wind speeds compared to the other directions.

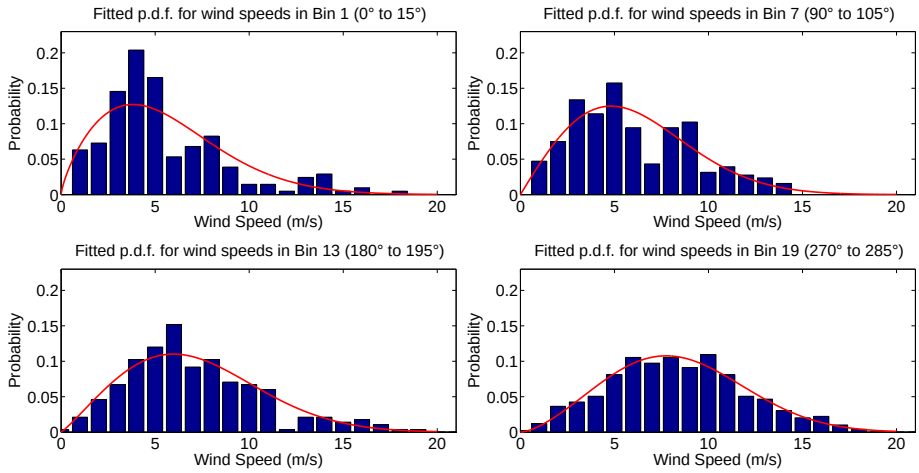


**Figure 7.2:** Distribution of the wind direction for the wind data from 2003.

## 7.2 Annual power production

The observations have been sorted in bins and Weibull distribution has been fitted to the wind speeds. This makes it possible to calculate the possibility for a certain wind speed from a given direction. To calculate the annual production

of a wind farm the possibility of a given wind speed and direction must be related to the the cumulated power production wind farm for the given the wind conditions. Therefore the cumulated power production, $\mathbf{P}_{cum}(U,\gamma)$, for a wind farm is formulated as a function of wind speed and direction.

$$\mathbf{P}_{cum}(U,\gamma) = \sum_{i=1}^{N} p(x_i^*, U_i, \gamma) \tag{7.3}$$

where $p(\mathbf{x}_i, U_i, \gamma)$ is the power production for turbine $i$ given the wind speed in front of turbine $U_i$ for wind direction $\gamma$. $x_i^*$ is the optimised set points for turbine $i$ for the given wind farm, at wind direction $\gamma$ and free wind speed $U$. Using the formulation of the cumulated power function and distribution of wind speed for each bin makes it possible to calculate the annual power production as:

$$\mathbf{P}_{annual} = 8760 \sum_{k=1}^{K} \left[ F_k \sum_{j=1}^{M} \left[ f(U_j^{int}; \theta_k^1, \theta_k^2) \mathbf{P}_{cum}\left(U_j^{int}, \gamma\right) \right] \left( \sum_{j=1}^{M} f(U_j^{int}; \theta_k^1, \theta_k^2) \right)^{-1} \right] \tag{7.4}$$

where $U^{int}$ is a vector of $M$ equidistant wind speed and $F_k$ is the probability that an observation belongs to bin $k$. The last term in the expression is a normalisation of the probability for a given wind speed in a bin. The result is multiplied with 8760 hours on a year. To calculate the annual production the optimised set points for a wind farm must be found of each wind speed in $U^{int}$ in each bin.

Each bin covers a range 15 degrees each which is a quite wide range considering the cumulated production for a wind speed can change a lot in this range, see Figure 5.4. The cumulated power function is calculated for three wind direction in each bin and the averaged value is used. E.g. the optimal set points has been calculated for direction 2.5°, 7.5°, and 12.5° for each wind speed in $U^{int}$ in bin 1. Since the optimal set point distribution repeats it self every 45° for square wind farm only nine different wind direction need to analysed. $U^{int}$ is the wind speeds from 0 to 25 m/s with steps of 1/3 m/s, meaning that 684 set points distribution should be optimised. As all turbines run on full load from 15 m/s the problems from 15 to 25 m/s are not actually solved as the optimal distribution is full load on all turbine. This counts for the wind speed between 0 and 3 m/s too, as this is below the cut-in speed. The reduced number of problems to be solved is 333.

The 333 problems have been solved for the 5x5 wind farm. Also the annual production using MPPT has been calculated. The two annual productions for

the two strategies are:

$$\mathbf{P}_{annual}^{\text{MPPT}} = 352560 \text{ MWh} \tag{7.5}$$

$$\mathbf{P}_{annual}^{\text{opt}} = 358796 \text{ MWh} \tag{7.6}$$

$$\mathbf{P}_{annual}^{\text{freeWind}} = 413613 \text{ MWh} \tag{7.7}$$

The annual production using the optimised set points are 1.77 % higher than using MPPT. The annual power production on the wind farm if wake effects were ignored is seen to be 413613 MWh, which is 14.76 % higher than the MPPT, meaning that wake effects reduce the power production with 13.25 % when the MPPT strategy i used. Curtailing turbines removes 11.98 % of the total wake effects, observed in the squared 5x5 wind farm annually.

The annual production for the fan-shaped 5x5 wind farm from Chapter 6 has also been calculated using same approach. Due to the shape of the wind farm 180 degrees of direction will have to be analysed meaning the number of problems to be solved is 1332 as the same step between angles is used. The annual production for the fan wind farm is:

$$\mathbf{P}_{annual}^{\text{MPPT}} = 360139 \text{ MWh} \tag{7.8}$$

$$\mathbf{P}_{annual}^{\text{opt}} = 363917 \text{ MWh} \tag{7.9}$$

Using the optimised set points gives an increase of 1.05% for the fan-shaped wind farm, which is 0.72% less than for the square wind farm. This is as expected since the wake effects only reduces the annual production 12.02 %. This result indicates that the fan shaped layout has reduced the wake effects compared to the squared layout.

The average spot price on energy for DK-West for 2014 was 228.63 DKK / MWh (data from: www.Energinet.dk). This means that the annual profit for curtailing turbines is 1.43 mill. DKK for the square wind farm and 0.864 mill. DKK for the the fan-shaped wind farm.

## 7.3 Optimising the direction of the wind warm

The optimal orientation for a given wind farm can also be analysed for the data set. Changing the wind direction for all observations gives the same change in annual production as turning the layout of the wind farm correspondingly. The annual production is calculated for the wind farm 360 times, where the wind direction is changed 1 degree each time. This gives the annual production as a function of the orientation of the wind farm. This has been done for both the

square and fan-shaped wind farm. The results can be seen on Figure 7.3. It is noticed that the results repeat them selves for the squared wind farm every 90 degrees as expected (the solutions are symmetric every 45 degrees but due to the non-uniform wind directions, different results are obtained depending on the order of the solution). The optimal orientation of the wind farms are in both cases 90 degrees (meaning they should be turned 90 degrees west. The square wind farm is actually place optimal, as turning the farm 90 degrees wont change the layout.

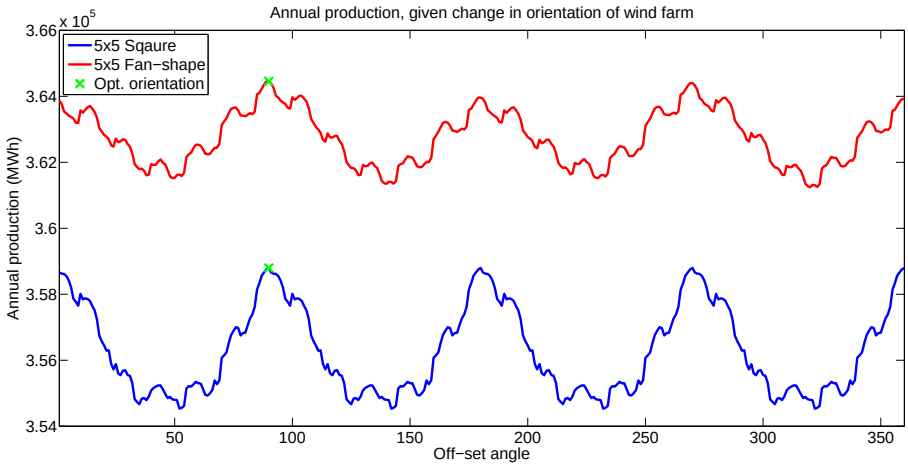


**Figure 7.3:** Distribution of the wind direction for the wind data from 2003.

Chapter 8

# Discussion

A control strategy, curtailing of upwind turbines, has been implemented to reduce wake effects in wind farms and compared with a strategy where losses to wake effects were accepted. The two strategies have been compared for two wind farm layouts. Curtailing performed better, or as good as MPPT for all wind directions and speeds (where all turbines were running). The performance of curtailing was very dependent on the wind direction and performed best in cases with intense wake effects. Forecasted weather data was used to calculate the annual production and curtailing improved the production with 1.77%. Strong wake effects for certain directions could be avoided, if the layout of the wind farm was fan shaped. This layout had an improved power production on 4.23% when using the MPPT strategy. The fan shaped layout reduced the production gain for curtailing to 1.05%. Considering these improvements, it should be noticed that they have been calculated for realised data, analysed in 15 degrees bins. The Jensen wake model has been shown to overestimate wake effects after the second downwind turbine. However, this was only seen when the range of the bins were smaller than 15% [GRB+12].

The objective function, used to optimise the set points, gave the optimiser converging problems. Several methods were proposed to give more robust solutions. Bundling downwind turbines performed almost as good as the reversed scan method but was much faster and gave more stable solutions. Perturbing the initial guesses gave the most robust solutions but had an increased run time.

The run time should be reduced for large wind farms, before the method could be tested on-site. Bundling turbines would be the recommended approach, as bundling reduces the number of set points to be optimised and run time.

Suggestions for future work would be to develop an algorithm that could detect patterns in the wake effects, for wind farms in two dimensions. This would allow bundling to be used in two dimensions. However, patterns were seen to be complex for the fan shaped wind farm. Analysing wake effects in patters or regions is also presented in Frandsen (2006) [FBP+06].

Testing the entire model's ability to fit data from a real wind farm could be an aim of future research. However, the wake model needs to be improved to handle non-stationary wind flows. The model could also be used to compare wind farm layouts, which was done in seconds using the MPPT strategy. The fan shaped wind farm improved the performance more than curtailing turbines did. An interesting field for future work could be to focus on optimising wind farm layouts instead of turbine control.

# Bibliography


[Ain88] J.F. Ainslie. Calculating the field in the wake of wind turbines. *Journal of Wind Engineering and Industrial Aerodynamics*, 27(1):213–224, 1988.

[ASJ+14] J. Annoni, P. Seiler, K. Johnson, P. Fleming, and P. Gebraad. Evaluating wake models for wind farm control. In *American Control Conference, Portland, OR, USA*, 2014.

[BRBA12] P. Beaucage, N. Robinson, M. Brower, and C. Alonge. Overview of six commerical and research wake models for large offshore wind farms. In *Proceedings of the European Wind Energy Association Conference*, pages 95–99, 2012.

[BWF10] A Bossanyi, A Wright, and P Fleming. Controller field tests on the nrel cart3 turbine. Report 11593/BR/09, National Renewable Energy Laboratory l, 2010.

[CC13] G. Crasto and F. Castellani. Wakes calculation in a offshore wind farm. *Wind Engineering*, 37(3):269–280, 2013.

[CHF99] A Crespo, J Hernandez, and S Frandsen. Survey of modelling methods for wind turbine wakes and wind farms. *Wind energy*, 2(1):1–24, 1999.

[FBP+06] S. Frandsen, R. Barthelmie, S. Pryor, O. Rathmann, S. Larsen, J. Højstrup, and M. Thøgersen. Analytical modelling of wind speed deficit in large offshore wind farms. *Wind energy*, 9(1-2):39–53, 2006.

[FG96] J. Fan and I. Gijbels. *Local polynomial modelling and its applications*. Chapman and Hall, 1996.

[FGC+14] P.A. Fleming, P.M.O. Gebraad, M.J. Churchfield, J.W. van Wingerden, A.K. Scholbrock, and P.J. Moriarty. Using particle filters to track wind turbine wakes for improved wind plant controls. In *American Control Conference (ACC), 2014*, pages 3734–3741, June 2014.

[GRB+12] M Gaumond, P. Réthoré, A. Bechmann, S. Ott, G. C. Larsen, A Peña, and K. S. Hansen. Benchmarking of wind turbine wake models in large offshore wind farms. In *Proceedings of the Science of Making Torque from Wind Conference*, 2012.

[GTvW+14] P.M.O. Gebraad, F.W. Teeuwisse, J.W. van Wingerden, P.A. Fleming, S.D. Ruben, J.R. Marden, and L.Y. Pao. A data-driven model for wind plant power optimization by yaw control. In *American Control Conference (ACC), 2014*, pages 3128–3134, June 2014.

[Han08] M.O.L. Hansen. *Aerodynamics of Wind Turbines*. Earthscan, second edition, 2008.

[JBMS09] J. M. Jonkman, S. Butterfield, W. Musial, and G. Scott. *Definition of a 5-MW reference wind turbine for offshore system development*. National Renewable Energy Laboratory Golden, CO, 2009.

[Jen83] N. O. Jensen. *A note on wind generator interaction*. 1983.

[KHJ86] I Katic, J Højstrup, and N.O. Jensen. A simple model for cluster efficiency. In *European Wind Energy Association Conference and Exhibition*, pages 407–410, 1986.

[Lar09] G. C. Larsen. A simple stationary semi-analytical wake model. In *Risø, Wind Energy Decision*, 2009.

[MBG+14] M. Mirzaei, T.G. Bozkurt, G. Giebel, P.E. Sørensen, and N.K. Poulsen. Estimation of the possible power of a wind farm. *International Federation of Automatic Control. World Congress. Proceedings*, 19:6782–6787, 2014.

[MSPN14] M. Mirzaei, M. Soltani, N.K. Poulsen, and H.H. Niemann. Model based active power control of a wind turbine. In *American Control Conference (ACC), 2014*, pages 5037–5042, 2014.

[New77] B.G. Newman. The spacing of wind turbines in large arrays. *Energy Conversion*, 16(4):169–171, 1977.

[San09] B. Sanderse. Aerodynamics of wind turbine wakes. *Energy Research Center of the Netherlands (ECN), ECN-E–09-016, Petten, The Netherlands, Tech. Rep*, 2009.

[VSC03] L.J. Vermeer, J. N. Sørensen, and A Crespo. Wind turbine wake aerodynamics. *Progress in aerospace sciences*, 39(6):467–510, 2003.

[WWY+12] C. Wan, J. Wang, G. Yang, H. Gu, and X. Zhang. Wind farm micro-siting by gaussian particle swarm optimization with local search strategy. *Renewable Energy*, 48:276–286, 2012.